

When inflationary perturbations refuse to classicalise: the role of non-Gaussianity in Wigner negativity

Aurora Ireland,^a Vincent Vennin^b

^a*Leinweber Institute for Theoretical Physics, Stanford University, Stanford, CA 94305, USA*

^b*Laboratoire de Physique de l'Ecole Normale Supérieure, ENS, CNRS, Université PSL, Sorbonne Université, Université Paris Cité, 75005 Paris, France*

E-mail: anireland@stanford.edu, vincent.vennin@phys.ens.fr

ABSTRACT: Inflationary perturbations are quantum in origin. Yet, when computing cosmological observables, they are often treated as classical stochastic fields. Do they nevertheless retain quantum birthmarks? A hallmark of genuinely quantum behaviour is quantum interferences, arising from phase coherence between distinct branches of the wavefunction. Such interference is diagnosed by the non-positivity of the Wigner function, and according to Hudson's theorem, the only pure states with positive Wigner functions are Gaussian states. Consequently, any departure from Gaussianity necessarily implies a non-positive Wigner function, precluding a description in terms of a classical distribution. This motivates us to compute the Wigner function of curvature perturbations, accounting for primordial non-Gaussianities, using the EFT of inflation. We find that the Wigner function develops pronounced interference fringes on super-Hubble scales, and in particular its negativity grows as a^2 in ultra-slow-roll backgrounds. These results demonstrate that quantum effects can remain significant at late times, and that squeezing alone does not ensure classicality, contrary to standard lore. This suggests that the prospects for detecting genuinely quantum signatures of the universe's origins in cosmological observables may be less bleak than previously thought.

Contents

1	Introduction	1
2	General formalism	5
2.1	EFT of inflation	5
2.2	Relating the Goldstone boson to the curvature perturbation	7
2.3	Canonical normalisation	8
2.4	Matching prescription	9
3	Constant-roll inflation	12
3.1	Wavefunction	12
3.2	Matching conditions	16
3.3	Wigner function	18
3.4	Comparison with linear theory	19
4	Results	22
4.1	Wigner oscillations and interference fringes	22
4.2	Wigner negativity	28
4.3	Parametric exploration	29
5	Discussion	30
A	Canonical transformations and boundary terms	33
A.1	Canonical transformations	33
A.2	Example: simplifying Eq. (2.6)	34
B	Additional plots	35
B.1	Negativity within the perturbative domain	35
B.2	Varying the coarse-graining parameter	36

1 Introduction

The leading paradigm for the formation of cosmic structure in our universe posits that it originates from quantum fluctuations of the vacuum during an early epoch of inflation [1–5]. As the comoving Hubble horizon shrinks, these fluctuations are stretched to super-Hubble scales, where they undergo parametric amplification. Later, following the end of inflation and a period of reheating, the perturbations re-enter the horizon during either radiation or matter domination, subsequently evolving into the density perturbations that seed the large-scale structure observed today. The predicted spectrum and statistical properties of

these perturbations [6–10] are in exceptional agreement with observations of the cosmic microwave background (CMB) anisotropies [11].

In this picture, inflationary perturbations are fundamentally quantum in origin. In practice, however, there are many contexts in which it is appropriate to treat these quantum fields as classical stochastic variables. In particular, two-point correlation functions can always be reproduced with a stochastic description [12]: one simply needs to consider a Gaussian random field whose covariance matrix matches the quantum two-point expectation values of the underlying quantum field. A standard approach in cosmology is thus to start from stochastic, Gaussian initial conditions at the end of inflation and evolve them as classical fields afterwards, according to the equations of cosmological perturbation theory. This standard practice raises two issues, however. First, at the practical level, it is not guaranteed that it properly captures higher-point statistics. Second, at the conceptual level, how a definite classical field configuration emerges from a quantum superposition of states remains elusive (this is the so-called quantum measurement problem).

Quantum-to-classical transition

The usual way to sidestep both problems and justify the replacement of quantum operators by classical stochastic fields is to assume that some sort of *quantum-to-classical transition* occurs at super-Hubble scales during inflation. Note that this transition is also essential to the stochastic approach to inflation [13], which provides an effective description of the long-wavelength modes by modeling the influence of shorter-wavelength fluctuations as an effective noise term. There are two main arguments in support of such a transition.

First, on super-Hubble scales the Heisenberg-picture curvature perturbation operator can be decomposed into a frozen mode and a decaying mode. The commutator between the curvature perturbation and its conjugate momentum, when compared with the anti-commutator, scales as the decaying mode, and hence becomes strongly suppressed. This has been argued to render the field and its momentum approximately commuting, and thus “classical” [14–18].¹ In the Schrödinger picture, this corresponds to quantum squeezing [19]: as the quantum state becomes localised along one phase-space direction, the squeezed direction becomes too suppressed to be measured, and the commutator cannot be accessed. However, this criterion is not invariant under field reparametrisations: by performing a phase-space rotation, the anti-commutator between the field and its momentum can always be made zero, contrary to the commutator whose size is fixed by \hbar . More generally, squeezing can always be undone by an appropriate linear canonical transformation [20], and hence it does not capture intrinsic (in technical terms, symplectic-invariant) properties of the quantum state [21].

Second, curvature perturbations do not form an isolated system: they may interact with other fields present in the early universe, becoming entangled with them. Even in the absence of other fields, gravitational self-interactions inevitably couple observable scales to inaccessible, small-wavelength modes [22]. There also exists entanglement in real space

¹This is sometimes referred to as “decoherence without decoherence”, although we shall avoid such terminology since cosmological perturbations are described by a pure (i.e. non-decohered) state in this approach.

between the spatial regions inside and outside our observable horizon [23]. When tracing over these environmental degrees of freedom, curvature perturbations need to be described by an open quantum system, subject to decoherence [24]. In the “pointer basis” selected by the interaction, quantum interferences become strongly suppressed [25], and the system effectively behaves as a statistical mixture of states, rather than a coherent superposition [22, 23, 26–38].

Can we prove that cosmic structures have a quantum-mechanical origin?

Even though decoherence does not solve the quantum measurement problem [39, 40], it erases some of the quantum signatures in primordial perturbations, making it difficult to establish whether cosmological structures are of quantum origin. In this work, we address this question while neglecting the role of decoherence for two main reasons. First, as we shall see, the framework we develop is already quite involved even for closed systems, and so we postpone the inclusion of environmental effects to future works in order to better organise the discussion. This also allows us to critically assess the role of squeezing (if any), which is already present at the pure-state level. Second, even if decoherence is effective, it does not necessarily imply that all quantum features are erased: as shown in [34], what matters is the *rate* at which decoherence proceeds, rather than the final amount.²

There have been several attempts to reveal the presence of genuine quantum features in primordial perturbations. These range from calculating entanglement measures such as quantum discord [12, 41], to constructing Bell [42–47] or Leggett-Garg [48, 49] inequalities, to searching for features in the primordial bispectrum [50–52]. These analyses reveal substantial entanglement between opposite Fourier modes, which are spontaneously created from the quantum vacuum. However, this does not lead to significant entanglement between disjoint regions of physical space [53–58]. This is because local measurements of quantum fields implicitly involve a trace over unobserved regions, resulting in decoherence that suppresses entanglement.³

Quantum interference and the Wigner function

For this reason, rather of attempting to reveal entanglement, in this work we focus on another hallmark of quantum theory: the presence of interferences. In phase space, quantum interferences are evidenced by Wigner negativity, which motivates us to now review the main properties of the Wigner function. For a quantum state described by the density matrix $\hat{\rho}$ on phase space (x, p) , the Wigner function is defined as the Wigner-Weyl transform of the density matrix [63]

$$W(x, p) = \frac{1}{2\pi} \int_{-\infty}^{\infty} du e^{-ipu} \left\langle x - \frac{u}{2} \middle| \hat{\rho} \middle| x + \frac{u}{2} \right\rangle. \quad (1.1)$$

Since the Wigner-Weyl transform is invertible, this provides a representation of the quantum state which is fully equivalent to the density matrix [64]. One of the reasons why this

²Concretely, in inflating spacetimes for decoherence to erase self-entanglement within curvature perturbations, purity needs to decay faster than a^{-4} , where a is the scale factor.

³This can be further interpreted as delocalisation of the partner mode [59–62].

representation is useful is that the expectation value of any operator \hat{O} can be written as

$$\langle \hat{O} \rangle = \text{Tr}(\hat{O}\hat{\rho}) = \int dx dp O(x, p) W(x, p), \quad (1.2)$$

where $O(x, p) = (2\pi)^{-1} \int du \langle x - u/2 | \hat{O} | x + u/2 \rangle$ is the Wigner-Weyl transform of \hat{O} . Since the Wigner function is real (given that $\hat{\rho}$ is Hermitian) and normalised to one ($\int dx dp W(x, p) = 1$, since $\text{Tr}(\hat{\rho}) = 1$), one may thus view W as a quasi-distribution function against which observables can be computed. The precautionary prefix “quasi” is a reminder that the Wigner function is not necessarily everywhere positive. When it is positive, the state may be viewed as classical in the sense that it can be represented by a distribution function describing stochastic processes in phase space.⁴ By contrast, regions of negativity in the Wigner function mark a departure from classical behaviour [69].

Wigner negativity provides a phase-space signature of the interferences arising from quantum superpositions. As an illustration, consider the quantum cat state

$$|\psi\rangle = \frac{1}{\sqrt{2}} (|\psi_1\rangle + |\psi_2\rangle), \quad (1.3)$$

where ψ_1 and ψ_2 are each Gaussian wavefunctions. The Wigner function of such a state is given by

$$W = \frac{1}{2} (W_1 + W_2) + W_{\text{int}}, \quad (1.4)$$

where W_1 and W_2 are the Wigner functions of ψ_1 and ψ_2 , respectively. While these are Gaussian, and hence everywhere positive, the cross-term

$$W_{\text{int}}(x, p) \propto \cos(\Delta\bar{x}p + \Delta\bar{p}x), \quad (1.5)$$

features interference fringes with alternating positive and negative regions, which encode phase coherence. In this expression, $\Delta\bar{x} = \langle \psi_1 | \hat{x} | \psi_1 \rangle - \langle \psi_2 | \hat{x} | \psi_2 \rangle$ and $\Delta\bar{p} = \langle \psi_1 | \hat{p} | \psi_1 \rangle - \langle \psi_2 | \hat{p} | \psi_2 \rangle$ denote the relative differences in mean position and momentum, respectively. If the state decoheres, then the density matrix reduces to a statistical mixture $\hat{\rho} \rightarrow (|\psi_1\rangle\langle\psi_1| + |\psi_2\rangle\langle\psi_2|)/2$, for which $W_{\text{int}} = 0$ and the Wigner function becomes strictly positive. For these reasons, Wigner negativity, defined as

$$\mathcal{N} = \frac{1}{2} \left[\int dx dp |W(x, p)| - 1 \right], \quad (1.6)$$

quantifies coherence between classically distinct configurations and is commonly used to monitor interference. In the context of resource theories, Wigner negativity is also a resource for quantum advantage [70].

⁴This led John Bell to argue in 1986 that states with positive Wigner functions cannot violate Bell inequalities [65]. In 2005, Revzen showed that this statement is correct only if Bell operators are constructed out of proper spin operators (i.e. operators whose Wigner-Weyl transform takes value within the operator’s spectrum), but that Bell inequality can otherwise be violated even if the Wigner distribution is positive definite [66, 67]. See [68] for a historical perspective on this issue, and [44] for explicit instances of Bell-inequality violations with positive Wigner functions and improper pseudo-spin operators.

The main motivation for this work comes from Hudson's theorem, which states that *a pure state has a non-negative Wigner function if and only if it is Gaussian* [71, 72]. As a contrapositive, any non-Gaussian pure state exhibits Wigner negativity.

This is where primordial fluctuations rejoin the discussion: at leading order in perturbation theory, they are described by a quadratic Hamiltonian, and so provided they are initiated in a Gaussian state (as in the Bunch-Davies vacuum), they remain Gaussian and the Wigner function remains positive. General Relativity being non-linear, at higher order in perturbation theory the Hamiltonian receives cubic and higher order corrections. These terms render the state non-Gaussian, and hence the Wigner function non-positive.

According to this reasoning, primordial fluctuations necessarily display quantum interferences, and the goal of this work is to make this statement explicit. The main difficulty is that, in regions of phase space where the inclusion of non-linearities makes the Wigner function negative, perturbative methods break down, since a change of sign always corresponds to large relative modifications. For this reason, non-perturbative methods must be employed. Here we choose to work with the effective field theory (EFT) of inflation, which we introduce in Sec. 2 together with a homogeneous matching procedure inspired by the separate-universe approach. In Sec. 3, we specialise to a general constant-roll background and solve for the wavefunction and Wigner function for the Goldstone of the EFT of inflation (which is closely related to the curvature perturbation). In Sec. 4, we present our results for the time evolution, parameter dependencies, and negativity of the Wigner function in an ultra-slow roll background. Finally, we conclude in Sec. 5 by discussing the implications of our results, as well as outlining a number of future directions.

2 General formalism

2.1 EFT of inflation

In order to capture non-Gaussian features in the quantum state of primordial perturbations, we need to go beyond linear cosmological perturbation theory, since in linear theory the Hamiltonian is quadratic and starting from the Bunch-Davies vacuum the Wigner function always remains Gaussian. One possibility is to work at higher order in cosmological perturbation theory, i.e. include cubic or higher terms in the action, since those lead to non-Gaussianities. However, to remain in the validity domain of the perturbative expansion, only small fractional modifications to the Wigner function can be studied with such an approach, and this excludes sign changes. This is why, in order to reveal potential non-positivity of the Wigner function, one needs to resort to non-perturbative techniques.

One such non-perturbative scheme is the Effective Field Theory (EFT) of inflation [73], which we briefly review. For simplicity, we consider a model of single-field inflation where the background inflaton field evolves according to some homogeneous solution $\phi_b(t)$. This background defines a preferred time-slicing and spontaneously breaks time translation invariance. As a result, inflaton perturbations $\delta\phi(t, \mathbf{x})$ transform non-linearly with respect to time diffeomorphisms,

$$t \rightarrow t + \xi^0(t, \mathbf{x}), \quad \delta\phi(t, \mathbf{x}) \rightarrow \delta\phi(t, \mathbf{x}) + \dot{\phi}_b(t)\xi^0(t, \mathbf{x}). \quad (2.1)$$

To construct an action for perturbations in this background, we first go to unitary gauge, where inflaton fluctuations vanish $\delta\phi = 0$ and all perturbations are encoded in the metric. In this gauge, $\delta\phi$ can be interpreted as having been eaten by the graviton, in analogy to how Goldstones are eaten by vector bosons in unitary gauge of spontaneously-broken gauge theories. We then write down all operators which respect the remaining unbroken spatial diffeomorphism, and finally restore full diffeomorphism invariance by promoting the parameter $\xi^0(x)$ to a field $\chi(x)$, which non-linearly realises the time-translation symmetry,

$$\chi(x) \rightarrow \chi(x) - \xi^0(x). \quad (2.2)$$

The field $\chi(x)$ should be interpreted as the Goldstone mode, which also describes scalar perturbations around the Friedmann-Lemaître-Robertson-Walker (FLRW) solution. The main advantage of re-introducing the Goldstone boson (rather than having it eaten) is that it makes the high-energy behaviour manifest. In particular, at high energies the mixing between the Goldstone and the graviton polarizations vanishes and so the two sectors decouple. Since mixing terms are suppressed by powers of the first slow-roll parameter ϵ_1 or $1/M_{\text{Pl}}^2$, where M_{Pl} is the reduced Planck mass, this scale can generally be quite low.⁵ Above it, we can study the physics of the Goldstone whilst neglecting metric fluctuations [74, 75].

In this so-called “decoupling” limit, a Hamiltonian that is valid to all orders in perturbation theory can be derived as follows [76]. Consider the action for the matter and gravitational sectors of an FLRW quasi-de Sitter inflationary background $S = S_{\text{matt}} + S_{\text{grav}}$, where S_{grav} is the usual Einstein-Hilbert action. In the decoupling limit, we neglect gravitational backreaction and treat the metric as unperturbed. In practice, this amounts to taking the ADM lapse and shift to be non-dynamical and trivial, $N = 1$ and $N^i = 0$. All perturbations are then encoded in the matter sector, and we can focus on the decoupled action for χ , which reads⁶ [73]

$$S = -M_{\text{Pl}}^2 \int d^4x a^3(t) \left\{ 3H^2(t + \chi) + 2(1 + \dot{\chi}) \dot{H}(t + \chi) + \dot{H}(t + \chi) \left[\dot{\chi}^2 - \frac{1}{a^2(t)} (\partial\chi)^2 \right] \right\}. \quad (2.3)$$

In this expression, time is labeled by cosmic time t , and H denotes the Hubble expansion rate, evaluated on the background solution. Notice that what appears in the argument of H is not t , but rather $t + \chi$, since this is the combination that transforms linearly under time translations. Notice also that all the interactions are encoded in the χ -dependence of the background dynamics.

This action can be simplified considerably by working to leading order in $\epsilon_1 \equiv -\dot{H}/H^2$, the so-called “decoupling limit” mentioned above. First, we can rewrite

$$\dot{H}(t + \chi) = -H^2(t + \chi)\epsilon_1(t + \chi) = -H^2(t)\epsilon_1(t + \chi) + \mathcal{O}(\epsilon_1^2). \quad (2.4)$$

Additionally, using that $H(t + \chi) - H(t) = \mathcal{O}(\epsilon_1)$, we can write

$$H^2(t + \chi) = \{H(t) + [H(t + \chi) - H(t)]\}^2 = 2H(t)H(t + \chi) - H^2(t) + \mathcal{O}(\epsilon_1^2). \quad (2.5)$$

⁵Formally, the decoupling limit corresponds to taking $M_{\text{Pl}}^2 \rightarrow \infty$ and $\epsilon_1 \rightarrow 0$ such that $M_{\text{Pl}}^2\epsilon_1 = \text{constant}$.

⁶This expression also assumes a canonically normalised and minimally coupled inflaton field with sound speed $c_s = 1$.

The first two terms in Eq. (2.3) can then be combined into a total derivative term, and the action can be rewritten as

$$S = M_{\text{Pl}}^2 \int d^4x a^3(t) H^2(t) \epsilon_1(t + \chi) \left[\dot{\chi}^2 - \frac{1}{a^2(t)} (\partial\chi)^2 \right] - M_{\text{Pl}}^2 \int d^4x \frac{d}{dt} [2a^3(t) H(t + \chi)] , \quad (2.6)$$

where we have dropped terms $\mathcal{O}(\epsilon_1^2)$ and higher, as well as a field-independent constant. The total-derivative term can be absorbed by performing the canonical transformation $\chi = \tilde{\chi}$ and $\pi = \tilde{\pi} + 2M_{\text{Pl}}^2 a^3(t) H^2(t) \epsilon_1(t + \tilde{\chi})$, as shown⁷ in Appendix A. We will use these transformed variables but drop the tildes for notational convenience. The result is the dramatically simplified action

$$S = M_{\text{Pl}}^2 \int d^4x a^3(t) H^2(t) \epsilon_1(t + \chi) \left[\dot{\chi}^2 - \frac{1}{a^2(t)} (\partial\chi)^2 \right] , \quad (2.7)$$

which matches the result of [76, 77]. Notice that χ no longer appears in the argument of H , but does appear in the argument of the first slow-roll parameter, $\epsilon_1(t + \chi)$.

2.2 Relating the Goldstone boson to the curvature perturbation

The Goldstone of broken time diffeomorphisms, χ , can be related to the comoving curvature perturbation \mathcal{R} as follows. In comoving gauge, the Goldstone vanishes and the comoving curvature perturbation enters in the spatial components of the metric h_{ij} as

$$\chi(t) = 0, \quad h_{ij}(t) = a^2(t) e^{2\mathcal{R}} \delta_{ij} . \quad (2.8)$$

Meanwhile in spatially flat gauge, the curvature perturbation vanishes $\mathcal{R} = 0$ but χ is finite,

$$\chi(\tilde{t}) \neq 0, \quad h_{ij}(\tilde{t}) = a(\tilde{t})^2 \delta_{ij} . \quad (2.9)$$

These two coordinate systems are related by a time diffeomorphism, $\tilde{t} = t + \xi_0$. By equating the metrics, we can solve for the curvature perturbation as [78–80]

$$\mathcal{R}(t, \mathbf{x}) = \ln \left[\frac{a(t + \xi_0)}{a(t)} \right] = \int_t^{t + \xi_0(t, \mathbf{x})} dt' H(t') . \quad (2.10)$$

Formally, this can be solved as

$$\mathcal{R} = \sum_{n=1}^{\infty} \frac{1}{n!} H^{(n-1)}(t) \xi_0^n , \quad (2.11)$$

where $H^{(n)} = \frac{d^n}{dt^n} H$, and in the decoupling limit this reduces to $\mathcal{R} = H \xi_0$.

Moreover, under a time diffeomorphism, recall that the Goldstone shifts according to Eq. (2.2). In particular in going from flat gauge to comoving gauge, we have $\chi(\tilde{t}) \rightarrow \chi(\tilde{t}) + \xi_0$. By equating this to the value of the Goldstone in comoving gauge $\chi(t) = 0$, we obtain the equation

$$\chi(t + \xi_0) + \xi_0 = 0 , \quad (2.12)$$

⁷As numerous canonical transformations are employed in this work, we present a full derivation of the first in this appendix and omit analogous steps in subsequent cases.

which implicitly relates ξ_0 to χ . A formal solution to this equation is given by

$$\xi_0(t) = \sum_{n=1}^{\infty} \frac{(-1)^n}{n!} [\chi^n(t)]^{(n-1)}, \quad (2.13)$$

which follows from an application of the Lagrange inversion theorem⁸. Combining this result with Eq. (2.11) and using the general Leibniz rule combined with the Cauchy product rule finally leads to the following non-linear relationship between \mathcal{R} and χ ,

$$\mathcal{R} = \sum_{n=1}^{\infty} \frac{(-1)^n}{n!} (H\chi^n)^{(n-1)}. \quad (2.15)$$

If the curvature perturbation is conserved, then in the decoupling limit $\xi^0 = \mathcal{R}/H$ is conserved too, and Eq. (2.12) implies that χ is conserved as well, and

$$\mathcal{R} = -H\chi. \quad (2.16)$$

Otherwise, the relation between χ and \mathcal{R} remains non-linear even in the decoupling limit. Note however that since the Lagrangian in Eq. (2.7) is proportional to $\partial_\mu \chi \partial^\mu \chi$, $\chi = \text{constant}$ always provides a solution to the complete non-linear equations of motion. This is why χ plays no less fundamental role than \mathcal{R} , and in what follows we will study its quantum state rather than the one of \mathcal{R} .

2.3 Canonical normalisation

Before solving for the quantum state of the Goldstone boson χ , let us see how the action in Eq. (2.7) can be rewritten in canonical form, i.e. with a canonical kinetic term. Focusing of the homogeneous mode $\chi_0(t)$, the Lagrangian is of the form

$$L(\chi_0, \dot{\chi}_0, t) = f(t, \chi_0) \dot{\chi}_0^2, \quad \text{with} \quad f(t, \chi_0) = \mathcal{V} M_{\text{Pl}}^2 a^3(t) H^2(t) \epsilon_1(t + \chi_0), \quad (2.17)$$

where $\mathcal{V} = \int d^3x$ is the comoving volume coming from the spatial integral in Eq. (2.7). Let us introduce the new variable

$$X(t, \chi_0) = \int_{\chi_{\text{ref}}}^{\chi_0} d\tilde{\chi} \sqrt{2f(t, \tilde{\chi})}, \quad (2.18)$$

where χ_{ref} is an arbitrary reference value. One has

$$\dot{X} = \sqrt{2f(t, \chi_0)} \dot{\chi}_0 + \int_{\chi_{\text{ref}}}^{\chi_0} d\tilde{\chi} \frac{\partial_t f(t, \tilde{\chi})}{\sqrt{2f(t, \tilde{\chi})}}, \quad (2.19)$$

⁸The Lagrange inversion theorem [81, 82] allows one to obtain the formal series expansion of an inverse function. Given an implicit equation of the form $y = t + af(y)$, one has the formal series solution

$$y(t) = t + \sum_{n=1}^{\infty} \frac{a^n}{n!} \frac{\partial^{n-1}}{\partial t^{n-1}} [f(t)^n]. \quad (2.14)$$

In order to apply this to solve Eq. (2.12), we perform the change of variables $y(t) = t + \xi_0(t)$, which brings the equation into the form $y = t - \chi(y)$. One can then use Eq. (2.14) with $a = -1$ to obtain the solution in Eq. (2.13).

such that the Lagrangian becomes

$$L(X, \dot{X}, t) = \frac{1}{2} \left[\dot{X} - A(t, X) \right]^2, \quad (2.20)$$

where we have defined

$$A(t, X) = \int_{\chi_{\text{ref}}}^{\chi_0(t, X)} d\tilde{\chi} \frac{\partial_t f(t, \tilde{\chi})}{\sqrt{2f(t, \tilde{\chi})}}, \quad (2.21)$$

and $\chi_0(t, X)$ denotes the inverse of $X(t, \chi_0)$. The term in L which is linear in \dot{X} can be removed by subtracting a total time derivative. We introduce

$$F(t, X) = \int_{X_{\text{ref}}}^X d\tilde{X} A(t, \tilde{X}), \quad (2.22)$$

the total time derivative of which is

$$\frac{d}{dt} F(t, X) = A(t, X) \dot{X} + \int_{X_{\text{ref}}}^X d\tilde{X} \frac{\partial}{\partial t} A(t, \tilde{X}). \quad (2.23)$$

By substituting the term $\dot{X} A(t, X)$ appearing in the Lagrangian with the expression above, one obtains

$$L(X, \dot{X}, t) = \frac{1}{2} \dot{X}^2 - V(t, X) - \frac{d}{dt} F(t, X), \quad (2.24)$$

where we have defined the potential

$$V(t, X) = -\frac{1}{2} A(t, X)^2 - \int_{X_{\text{ref}}}^X d\tilde{X} \frac{\partial}{\partial t} A(t, \tilde{X}). \quad (2.25)$$

The total derivative term can be removed by performing the canonical transformation $X = \tilde{X}$, $\pi_X = \tilde{\pi}_X - A(t, X)$, as we demonstrate in Appendix A. The Lagrangian is thus cast in a form where the kinetic term is canonical,

$$L(X, \dot{X}, t) = \frac{1}{2} \dot{X}^2 - V(t, X), \quad (2.26)$$

although it now contains a time-dependent self-interaction potential $V(t, X)$.

2.4 Matching prescription

The canonical Lagrangian (2.26) describes the dynamics of the homogeneous mode⁹ $\chi_0(t)$; hence it only applies to cosmological fluctuations whose spatial extent λ far exceeds the Hubble radius, $\lambda < \lambda_\sigma \equiv (\sigma H)^{-1}$, where $\sigma \ll 1$. At near- and sub-Hubble scales, keeping track of the quantum state of χ is more involved since it requires solving the Schrödinger equation for a wavefunctional, rather than a wavefunction. This is why, in this work, we will adopt the same strategy as in the δN formalism [83–87] or the stochastic- δN formalism [88–90], where perturbation theory is employed within λ_σ , and above λ_σ one uses the

⁹The “homogeneous mode” $\chi_0(t)$ should be understood as a proxy for some appropriately coarse-grained long-wavelength field, rather than as the literal global homogeneous field configuration. Equivalently, $\chi_0(t)$ can be interpreted as the leading-order term in the gradient expansion.

separate-universe approach [85, 91–95], according to which the universe can be described as a collection of independent FLRW patches. This implies that the results derived below only account for non-linearities at large scales, which are nonetheless expected to be the most relevant ones since, inside the Hubble radius, cosmological fluctuations are not subject to the parametric amplification driven by the background expansion, and thus remain close to their vacuum Gaussian state.

The above scheme implies that a matching procedure is enforced at the scale λ_σ , in order to set initial conditions for the homogeneous-mode Schrödinger equation. In practice, we consider fluctuations with a physical wavelength λ (or equivalently, with comoving wavenumber $k = a/\lambda$), and we denote by t_\star the time at which $k = \sigma a_\star H$. Since linear perturbation theory is employed to describe the phase $t < t_\star$, at time t_\star the wavefunction of X is still Gaussian,¹⁰

$$\psi_X(t, X) = N(t) e^{-\alpha(t)X^2} \quad \text{for } t \leq t_\star, \quad (2.27)$$

where $|N| = (2\alpha_R/\pi)^{1/4}$ for the state to be properly normalized. The wavefunction being Gaussian, the parameter $\alpha = \alpha_R + i\alpha_I$ is entirely determined by the quadratic moments of X and its conjugate momentum π_X ,

$$\begin{aligned} \langle \hat{X}^2 \rangle &= \frac{1}{4\alpha_R}, \\ \langle \hat{\pi}_X^2 \rangle &= \frac{|\alpha|^2}{\alpha_R}, \\ \langle \hat{X} \hat{\pi}_X \rangle &= \frac{i}{2} - \frac{\alpha_I}{2\alpha_R}, \end{aligned} \quad (2.28)$$

where we have used the representation $\hat{\pi}_X = -i\partial_X$ for the conjugate momentum. The above can be readily inverted to find

$$\alpha = -\frac{i}{2} \frac{\langle \hat{X} \hat{\pi}_X \rangle}{\langle \hat{X}^2 \rangle}. \quad (2.29)$$

Meanwhile, from linear perturbation theory one can compute the power spectra $\mathcal{P}_{XX}(t, k)$, $\mathcal{P}_{\pi\pi}(t, k)$, and $\mathcal{P}_{X\pi}(t, k)$, where in general we define the power spectrum \mathcal{P}_{gh} for the fields \hat{g} and \hat{h} as

$$\frac{k^3}{2\pi^2} \langle \hat{g}_{\mathbf{k}} \hat{h}_{\mathbf{k}'}^\dagger \rangle = \mathcal{P}_{gh}(k) \delta^{(3)}(\mathbf{k} - \mathbf{k}'). \quad (2.30)$$

In real space, $\langle \hat{g}(\mathbf{x}) \hat{h}(\mathbf{x}) \rangle = \bar{g}\bar{h} + \int d\ln k \mathcal{P}_{hg}(k)$, where $\bar{g} \equiv \langle \hat{g}(\mathbf{x}) \rangle$ is the (possibly non-vanishing) one-point function. As described above, our goal is to describe fluctuations at a given comoving scale k , employing perturbation theory before a certain matching time and the homogeneous-mode description afterwards. The matching can thus be performed by identifying the two-point functions of the quantised homogeneous field operators $\hat{\chi}_0$ and

¹⁰More generally, the wavefunction is of the form $\psi_X = N e^{-\alpha(X - \bar{X})^2}$, where a non-zero \bar{X} allows for a non-vanishing $\langle \hat{X} \rangle$ and $\langle \hat{\pi}_X \rangle$. For our choice of reference point $\chi_{\text{ref}} = 0$, $\bar{X} = 0$ at linear order.

$\hat{\pi}_0$ with their linear power spectra as¹¹

$$\begin{aligned}\langle \hat{\chi}_0^2 \rangle &\rightarrow \bar{\chi}_0^2 + \mu_1 \mu_2 \mathcal{P}_{\chi\chi}(t_\star, k), \\ \langle \hat{\chi}_0 \hat{\pi}_0 \rangle &\rightarrow \bar{\chi}_0 \bar{\pi}_0 + \mu_1 \mathcal{P}_{\chi\pi}(t_\star, k), \\ \langle \hat{\pi}_0^2 \rangle &\rightarrow \bar{\pi}_0^2 + \frac{\mu_1}{\mu_2} \mathcal{P}_{\pi\pi}(t_\star, k).\end{aligned}\tag{2.31}$$

Two parameters appear in this identification, which play different roles [53]. The first, μ_1 , must be chosen such that the homogeneous fields χ_0 and π_0 are canonically normalised, i.e. $\langle [\hat{\chi}_0, \hat{\pi}_0] \rangle = 2i\text{Im}[\langle \hat{\chi}_0 \hat{\pi}_0 \rangle] = i$. Since the Fourier modes $\hat{\chi}_\mathbf{k}$ and $\hat{\pi}_\mathbf{k}$ are canonically normalised, $[\hat{\chi}_\mathbf{k}, \hat{\pi}_{\mathbf{k}'}^\dagger] = i\delta^{(3)}(\mathbf{k} - \mathbf{k}')$, one has $\text{Im}[\mathcal{P}_{\chi\pi}(k)] = k^3/4\pi^2$, which leads to

$$\mu_1 = \frac{2\pi^2}{k^3}.\tag{2.32}$$

This is also a natural choice for the comoving volume factor \mathcal{V} , since the homogeneous mode is extracted by coarse graining the field over an effective volume $\mathcal{V} \sim k^{-3}$. Though the precise relation between $\mu_1 = 2\pi^2/k^3$ and \mathcal{V} will depend on the window function chosen for the coarse graining (see [53]), they should be proportional up to some $\mathcal{O}(1)$ geometrical factor. Since the choice of this factor will not affect any physical observables, we set $\mathcal{V} = \mu_1$ without loss of generality. The second parameter, μ_2 , sets the units in which χ_0 and π_0 are measured. Because of the form of the Lagrangian (2.17), χ_0 has inverse-mass dimension,¹² and hence μ_2 must have the dimension of an inverse comoving volume. A natural choice is then

$$\mu_2 = \frac{1}{\mathcal{V}} = \frac{1}{\mu_1}.\tag{2.33}$$

Ultimately, since changing μ_2 simply amounts to performing a linear canonical transformation, which does not affect the properties discussed in Sec. 4 (in particular, the Wigner negativity), we adopt Eq. (2.33) without loss of generality.

Moreover, linearising Eq. (2.18) gives $X = \sqrt{2f(t, 0)} \chi_0$ provided we set $\chi_{\text{ref}} = 0$. This will be our convention going forward since, as discussed in footnote 10, this is the unique choice for which $\langle \hat{X} \rangle$ vanishes at linear order, greatly simplifying the matching conditions. From Eq. (2.26), one has $\pi_X = \dot{X}$, and from Eq. (2.17), $\pi_0 = 2f(t, 0)\dot{\chi}_0$. The conjugate momenta are then related as $\pi_X = [\pi_0 + \dot{f}(t, 0)\chi_0]/\sqrt{2f(t, 0)}$ at linear order. Together with Eqs. (2.29) and (2.31), this leads to

$$\alpha_\star = -\frac{i}{4} \frac{\dot{f}(t_\star, 0)}{f(t_\star, 0)} - \frac{i}{4} \frac{\mathcal{V}}{f(t_\star, 0)} \frac{\mathcal{P}_{\chi\pi}(t_\star, k)}{\mathcal{P}_{\chi\chi}(t_\star, k)},\tag{2.34}$$

where $\alpha_\star \equiv \alpha(t_\star)$. Introducing the second Hubble-flow parameter $\epsilon_2 \equiv \dot{\epsilon}_1/H\epsilon_1$, the first term can be evaluated by noting that $\dot{f}(t, 0)/f(t, 0) = (3 + \epsilon_2)H$. The second term can

¹¹We emphasise that $\bar{\chi}_0 \equiv \langle \hat{\chi}_0 \rangle$ and $\bar{\pi}_0 \equiv \langle \hat{\pi}_0 \rangle$ are quantum expectation values, not spatial averages.

¹²From Eqs. (2.7) and (2.17), we see that $\chi_0(t)$ and $\chi(t, \mathbf{x})$ have the same mass dimension. The same cannot be true for $\pi_0(t)$ and $\pi(t, \mathbf{x})$, since $[\chi_0, \pi_0] = i$ is dimensionless while $[\chi(\mathbf{x}), \pi(\mathbf{x}')] = i\delta(\mathbf{x} - \mathbf{x}')$ has the dimension of an inverse comoving volume. Another way to see why π_0 and π do not have the same dimension is to note that π_0 is defined with respect to the Lagrangian as $\pi_0 = \partial L/\partial \dot{\chi}_0$ whereas π is defined with respect to the Lagrangian *density* \mathcal{L} , $\pi = \partial \mathcal{L}/\partial \dot{\chi}$. Explicitly, $[\chi_0] = [\chi] = M^{-1}$ while $[\pi_0] = M$ and $[\pi] = M^4$.

be re-written in terms of power spectra of the curvature perturbation, which can be more easily computed in cosmological perturbation theory. Linearising Eq. (2.15) to obtain $\mathcal{R} = -H\chi$ and also noting that the momentum conjugate to the full field χ in Eq. (2.7) is $\pi \equiv \partial\mathcal{L}/\partial\dot{\chi} = 2f(t_*, 0)\dot{\chi}/\mathcal{V}$, we have $\mathcal{P}_{\mathcal{R}\mathcal{R}} = H^2\mathcal{P}_{\chi\chi}$ and $\mathcal{P}_{\mathcal{R}\dot{\mathcal{R}}} = [H^2\mathcal{V}/2f(t, 0)]\mathcal{P}_{\chi\pi}$. Thus, Eq. (2.34) becomes

$$\alpha_* = -\frac{i}{4}(3 + \epsilon_2)H - \frac{i}{2}\frac{\mathcal{P}_{\mathcal{R}\dot{\mathcal{R}}}(t_*, k)}{\mathcal{P}_{\mathcal{R}\mathcal{R}}(t_*, k)}, \quad (2.35)$$

where conveniently one notes that the factor of \mathcal{V} has cancelled out.

In linear perturbation theory, the mode function for the comoving curvature perturbation satisfies

$$\mathcal{R}_k'' + 2\frac{z'}{z}\mathcal{R}_k' + k^2\mathcal{R}_k = 0, \quad (2.36)$$

where primes denote derivatives with respect to conformal time $\eta = \int dt/a$ and $z^2 = 2M_{\text{Pl}}^2a^2\epsilon_1$ is the usual Mukhanov-Sasaki pump field, which governs the coupling of scalar perturbations to the background evolution. Upon solving this equation with appropriately chosen vacuum conditions, the power spectra in Eq. (2.35) can be evaluated according to $\mathcal{P}_{\mathcal{R}\dot{\mathcal{R}}}/\mathcal{P}_{\mathcal{R}\mathcal{R}} = \dot{\mathcal{R}}_k^*/\mathcal{R}_k^*$.

3 Constant-roll inflation

Let us now show how the Wigner function of the Goldstone boson χ_0 can be derived in the above framework. For concreteness, we consider a phase of inflation where the second Hubble-flow parameter $\epsilon_2 = \dot{\epsilon}_1/H\epsilon_1$ is constant. A constant value for ϵ_2 leads to a very simple time dependence for the first Hubble-flow parameter ϵ_1 , which will allow us to carry out explicit calculations. This regime is often referred to as “constant-roll” inflation, and it encompasses the well-known cases of slow roll (SR) for $\epsilon_2 = 0$ [96–99] and ultra-slow roll (USR) for $\epsilon_2 = -6$ [100–104].

3.1 Wavefunction

If ϵ_2 is constant, then in the decoupling limit one has

$$\epsilon_1(t) = \bar{\epsilon}_1 e^{\epsilon_2 H t}, \quad (3.1)$$

with $\bar{\epsilon}_1$ the value of ϵ_1 at a reference time $t = 0$, where we also set $a(0) = 1$. We take this reference to correspond to Hubble crossing, i.e. $k = aH|_{t=0} = H$, such that $\bar{\epsilon}_1$ denotes the value of ϵ_1 at horizon re-entry. The function f introduced in Eq. (2.17) then reads

$$f(t, \chi_0) = \mathcal{V}M_{\text{Pl}}^2H^2\bar{\epsilon}_1 e^{(3+\epsilon_2)Ht}e^{\epsilon_2 H\chi_0}, \quad (3.2)$$

where we have used that $a(t) = e^{Ht}$ in the decoupling limit. This function is separable in the sense that the t and χ_0 dependence in $\epsilon_1(t + \chi_0)$ factorises, which allows for dramatic simplifications in the procedure outlined in Sec. 2.3. In particular, Eqs. (2.18) and (2.21) lead to $A = \frac{1}{2}(3 + \epsilon_2)HX$, and so the potential (2.25) reads

$$V(t, X) = -\frac{1}{8}(3 + \epsilon_2)^2H^2X^2. \quad (3.3)$$

That this potential is quadratic in X implies that it admits Gaussian solutions, while non-Gaussian features are contained in the non-linear canonical transformation between χ_0 and X . One also notes that this potential is the same for SR ($\epsilon_2 = 0$) and USR ($\epsilon_2 = -6$) backgrounds, which is a manifestation of the Wands duality [105].

Though this potential is simple, time-independent, and quadratic, the change of variables relating X and χ_0 will introduce a time-dependent boundary condition which complicates solving the Schrödinger equation. In anticipation of simplifying this boundary condition, we will take a slight variation on the change of variables presented in Sec. 2.3. It should be relatively straightforward to map the previous results onto this new variable. With this motivation in mind, we factorise out the time dependence in f as

$$f(t, \chi_0) = e^{(3+\epsilon_2)Ht} g(\chi_0), \quad g(\chi_0) = \mathcal{V} M_{\text{Pl}}^2 H^2 \bar{\epsilon}_1 e^{\epsilon_2 H \chi_0}, \quad (3.4)$$

and introduce the change of variables

$$Y(\chi_0) = \int_0^{\chi_0} d\tilde{\chi} \sqrt{2g(\tilde{\chi})}, \quad (3.5)$$

where as in Sec. 2.4 we have set $\chi_{\text{ref}} = 0$. This is analogous to the definition of X in Eq. (2.18), but crucially because $g(\chi_0)$ is time-independent, $\dot{Y} = \sqrt{2g(\chi_0)} \dot{\chi}_0$ has no auxiliary A -piece. The Lagrangian is thus

$$L(Y, \dot{Y}, t) = \frac{1}{2} e^{(3+\epsilon_2)Ht} \dot{Y}^2. \quad (3.6)$$

While the kinetic term is not canonical, and therefore $\pi_Y = e^{(3+\epsilon_2)Ht} \dot{Y}$ has a time-dependent¹³ pre-factor, this brings no additional complications and can be accommodated by only a slight modification to the matching conditions.

Explicitly, the change of variables in Eq. (3.5) reads

$$Y = \frac{2\kappa}{\epsilon_2 H} \left(e^{\frac{1}{2}\epsilon_2 H \chi_0} - 1 \right), \quad \kappa = \sqrt{2\mathcal{V} M_{\text{Pl}}^2 H^2 \bar{\epsilon}_1}. \quad (3.7)$$

Notice that this relationship is generically non-linear, but reduces to linear for SR, $Y_{\text{SR}} = \kappa \chi_0$. Note also that unless $\epsilon_2 = 0$, this is a compactifying change of variables, with the domain $\chi_0 \in (-\infty, \infty)$ mapped to

$$Y \in \begin{cases} (-\infty, Y_b) & \epsilon_2 < 0, \\ (Y_b, \infty) & \epsilon_2 > 0, \end{cases} \quad (3.8)$$

where we have defined the finite boundary location

$$Y_b = -\frac{2\kappa}{\epsilon_2 H}. \quad (3.9)$$

¹³One can eliminate this time dependence by introducing a new time coordinate $\tau = -e^{-(3+\epsilon_2)Ht}/(3 + \epsilon_2)H$, in terms of which the kinetic term becomes canonical. Because we have already introduced enough new variables, and because this method offers no real computational simplification, we will not do so here.

We focus on the former case $\epsilon_2 < 0$ without loss of generality. As Y approaches Y_b , χ_0 approaches infinity, where its wavefunction must vanish for the quantum state to be normalisable. We therefore impose the Dirichlet boundary condition

$$\psi_Y(Y_b) = 0. \quad (3.10)$$

Note that the Gaussian ansatz used in the matching prescription of Sec. 2.4 does not satisfy this boundary condition. This mismatch is not problematic, however; the finite boundary is fundamentally a non-perturbative effect, whereas the matching condition is derived entirely within perturbation theory. In linear theory, using that $\langle \hat{Y}^2 \rangle = \kappa^2 \langle \hat{\chi}_0^2 \rangle \rightarrow (\kappa^2/H^2) \mathcal{P}_{\mathcal{R}\mathcal{R}}(t_*, k)$, one finds

$$\left. \frac{\langle \hat{Y}^2 \rangle}{Y_b^2} \right|_{t=t_*} = \frac{\epsilon_2^2}{4} \mathcal{P}_{\mathcal{R}\mathcal{R}}(t_*, k). \quad (3.11)$$

Since the power spectrum must be small for perturbation theory to be valid prior to the matching time, the ratio of $\langle \hat{Y}^2 \rangle$ to Y_b^2 must be small, ensuring that Y_b lies in the far tail of the wavefunction. The finite boundary is thus irrelevant to the linear-theory dynamics. Boundary effects and other non-perturbative features become important only afterwards, and it is precisely these phenomena that the super-Hubble homogeneous-mode description is intended to capture.

Since the Hamiltonian $H = \frac{1}{2}e^{-(3+\epsilon_2)Ht} \pi_Y^2$ is quadratic, the Schrödinger equation $i\partial_t \psi_Y = \hat{H} \psi_Y$ admits Gaussian solutions. The simplest ansatz consisting of Gaussian wavepackets which satisfies the boundary condition (3.10) is

$$\psi_Y(t, Y) = N(t) \left[e^{-\beta(t)Y^2} - e^{-\beta(t)(Y-2Y_b)^2} \right] \Theta(Y_b - Y), \quad (3.12)$$

where Θ is the Heaviside theta function restricting the domain to $Y \in (-\infty, Y_b)$. This approach, sometimes referred to as the ‘‘method of images’’ [106], is standard when describing Gaussian wavepackets incident on an infinite potential step in quantum mechanics. The second Gaussian can be interpreted as a reflection of the first wavepacket when it reaches the boundary. Since the ansatz (3.12) consists of a linear superposition of two Gaussians, it will be a solution provided each individual Gaussian satisfies the Schrödinger equation.

Substituting Eq. (3.12) into the Schrödinger equation yields the following differential equation for the complex parameter β ,

$$\dot{\beta} = -2ie^{-(3+\epsilon_2)Ht} \beta^2, \quad (3.13)$$

or equivalently for the real $\beta_R \equiv \text{Re}[\beta]$ and imaginary $\beta_I \equiv \text{Im}[\beta]$ parts

$$\dot{\beta}_R = 4e^{-(3+\epsilon_2)Ht} \beta_R \beta_I, \quad \dot{\beta}_I = -2e^{-(3+\epsilon_2)Ht} (\beta_R^2 - \beta_I^2). \quad (3.14)$$

Eq. (3.13) has the form of a Riccati equation, and can be solved by letting $\beta = -ie^{(3+\epsilon_2)Ht} \dot{\gamma}/2\gamma$. The equation for γ then takes the form $\ddot{\gamma} + (3 + \epsilon_2)H\dot{\gamma} = 0$, which is the classical Euler-Lagrange equation corresponding to the Lagrangian of Eq. (3.6). The general solution is $\gamma = c_1 + c_2 e^{-(3+\epsilon_2)H(t-t_*)}$, and using the initial condition $\beta(t_*) \equiv \beta_*$, one finds

$$\beta(t) = \frac{\beta_*}{1 - \frac{2i\beta_*}{(3+\epsilon_2)H} [e^{-(3+\epsilon_2)Ht} - e^{-(3+\epsilon_2)Ht_*}]} \cdot \quad (3.15)$$

The explicit form of β_\star will be derived in Sec. 3.2.

Upon substituting Eq. (3.12) into the Schrödinger equation, one also obtains the differential equation for the norm

$$\frac{\dot{N}}{N} = -ie^{-(3+\epsilon_2)Ht}\beta. \quad (3.16)$$

Meanwhile, in order for the wavefunction to be properly normalised, one must have

$$|N(t)| = \left(\frac{2\beta_R}{\pi} \right)^{1/4} \left(1 - e^{-2\frac{|\beta|^2}{\beta_R} Y_b^2} \right)^{-1/2}, \quad (3.17)$$

where β_R is required to be positive. One can verify that this solution also satisfies Eq. (3.16) since $|\dot{N}|/|N| = \dot{\beta}_R/4\beta_R = e^{-(3+\epsilon_2)Ht}\beta_I$, where we have used the equation of motion for β_R as well as the fact that $|\beta|^2/\beta_R$ is a constant in time, which may be seen by differentiating $\partial_t(|\beta|^2/\beta_R)$ and using the equations of motion in Eq. (3.14).

We can now transform back to the original variables χ_0 and π_0 as follows. The relationship between Y and χ_0 is given in Eq. (3.7), while from Eq. (3.6) the momentum conjugate to Y is $\pi_Y = e^{(3+\epsilon_2)Ht}\dot{Y}$ and from Eq. (2.17) the momentum conjugate to χ_0 is $\pi_0 = \kappa^2 e^{(3+\epsilon_2)Ht} e^{\epsilon_2 H \chi_0} \dot{\chi}_0$.¹⁴ Thus, we have

$$Y = \underbrace{\frac{2\kappa}{\epsilon_2 H} \left(e^{\frac{1}{2}\epsilon_2 H \chi_0} - 1 \right)}_{h(\chi_0)}, \quad \pi_Y = \underbrace{\frac{1}{\kappa} e^{-\frac{1}{2}\epsilon_2 H \chi_0} \pi_0}_{\pi_0/h'(\chi_0)}, \quad (3.18)$$

where ' denotes a derivative with respect to χ_0 . This transformation is of the form $Y = h(\chi_0)$ and $\pi_Y = \pi_0/h'(\chi_0)$, which manifestly preserves the Poisson-bracket structure. At the quantum mechanical level, the expression for π_Y should be Weyl-ordered according to $\hat{\pi}_Y = \frac{1}{2} \left[\frac{1}{h'(\hat{\chi}_0)} \hat{\pi}_0 + \hat{\pi}_0 \frac{1}{h'(\hat{\chi}_0)} \right]$ in order for π_Y to be Hermitian. Using that $\hat{\pi}_0 = -i \frac{\partial}{\partial \chi_0}$ in the position representation, the Weyl-ordered operator can equivalently be written as $\hat{\pi}_Y = \frac{1}{h'(\hat{\chi}_0)} \hat{\pi}_0 + \frac{i}{2} \frac{h''(\hat{\chi}_0)}{h'(\hat{\chi}_0)^2}$. At the operator level, the transformation then reads

$$\hat{Y} = h(\hat{\chi}_0), \quad \hat{\pi}_Y = \frac{1}{h'(\hat{\chi}_0)} \hat{\pi}_0 + \frac{i}{2} \frac{h''(\hat{\chi}_0)}{h'(\hat{\chi}_0)^2}, \quad (3.19)$$

and the wavefunction transforms under it according to [107]

$$\psi_0(\chi_0) = \sqrt{|h'(\chi_0)|} \psi_Y[h(\chi_0)], \quad (3.20)$$

where ψ_Y is given in Eq. (3.12). One can check that this transformation both preserves probability $|\psi_Y(Y)|^2 dY = |\psi_0(\chi_0)|^2 d\chi_0$ and ensures that $\hat{\pi}_0$ acts as the canonical momentum operator conjugate to χ_0 , i.e. $\hat{\pi}_0 \psi_0 = -i \frac{\partial}{\partial \chi_0} \psi_0$.

¹⁴For consistency with Sec. (2.4), we use here the conjugate momentum corresponding to the action in Eq. (2.7) rather than that in Eq. (2.6). The canonical transformation that eliminates the total derivative term from the action (2.7) amounts to shifting the conjugate momentum so as to eliminate its 1-point function. Working from this action then has the nice property that the Wigner function will be centred in phase space.

Writing out the wavefunction explicitly, one finds

$$\begin{aligned}\psi_0(\chi_0) &= \left(\frac{2\kappa^2\beta_R}{\pi}\right)^{1/4} \left(1 - e^{-2\frac{|\beta|^2}{\beta_R}Y_b^2}\right)^{-1/2} e^{\frac{1}{4}\epsilon_2 H \chi_0} \\ &\times \left(\exp\left[-\beta Y_b^2 \left(e^{\frac{1}{2}\epsilon_2 H \chi_0} - 1\right)^2\right] - \exp\left[-\beta Y_b^2 \left(e^{\frac{1}{2}\epsilon_2 H \chi_0} + 1\right)^2\right]\right),\end{aligned}\quad (3.21)$$

where the first line comes from the normalisation and Jacobian factors, the second line comes from substituting the non-linear relationship (3.7) in the Gaussian wavepackets of (3.12), and we have also used $Y_b = -2\kappa/\epsilon_2 H$. Due to the non-linear relationship between Y and χ_0 , the wavefunction for χ_0 is generically non-Gaussian. In the SR case, one may take the limit $\epsilon_2 \rightarrow 0$, for which $Y_b \rightarrow \infty$, to find

$$\psi_0^{\text{SR}}(\chi_0) = \left(\frac{2\kappa^2\beta_R}{\pi}\right)^{1/4} \exp(-\kappa^2\beta\chi_0^2), \quad (3.22)$$

which is simply a complex Gaussian. This occurs because in the SR limit the mapping between the variables χ_0 and Y reduces to linear.

3.2 Matching conditions

If ϵ_2 is constant, the general solution of Eq. (2.36) is

$$\mathcal{R}_k(\eta) = \sqrt{\frac{\pi}{2}} \frac{H}{\sqrt{2M_{\text{Pl}}^2\epsilon_1}} \frac{(-k\eta)^{3/2}}{\sqrt{2k^3}} \left[A_k H_\nu^{(1)}(-k\eta) + B_k H_\nu^{(2)}(-k\eta)\right], \quad (3.23)$$

where $H_\nu^{(1)}(x)$ and $H_\nu^{(2)}(x)$ are Hankel functions of the first and second kind, respectively, and $\nu = |3 + \epsilon_2|/2$. The Bogoliubov coefficients A_k and B_k should be normalised as $|A_k|^2 - |B_k|^2 = 1$ in order for $\hat{\mathcal{R}}_k$ and its conjugate momentum to satisfy the canonical commutation relations. Imposing the Bunch-Davies vacuum conditions in the asymptotic past amounts to setting $A_k = 1$ and $B_k = 0$, but in principle other Bogoliubov coefficients may be considered. Indeed, constant-roll periods with $\epsilon_2 < 0$ cannot extend indefinitely into the past since the first Hubble-flow parameter $\epsilon_1 \propto |\eta|^{-\epsilon_2}$ would grow without bound as $\eta \rightarrow -\infty$, eventually violating the condition for inflation ($\epsilon_1 < 1$).

In that case, we imagine that while the modes of interest were still sub-Hubble, there existed an initial slow-roll period which transitioned to constant roll at some η_t . We demand that this transition occur prior to the matching time $\eta_t < \eta_*$ such that the background is described by constant-roll dynamics for the entirety of the phase described by the homogeneous mode dynamics. While perturbations originate in the Bunch-Davies vacuum during the initial slow-roll phase, the transition to constant roll may excite the state, and from the perspective of the homogeneous mode description, the initial conditions will then look like an excited vacuum state with $B_k \neq 0$. If $\eta_t \ll \eta_*$, i.e. for modes that are deeply sub-Hubble at the time of the transition, one recovers $A_k = 1$ and $B_k = 0$ [108]. Nevertheless, we leave the Bogoliubov coefficients arbitrary at this point for maximal generality.

From Eqs. (2.30) and (3.23), the power spectra are

$$\begin{aligned}\mathcal{P}_{\mathcal{R}\mathcal{R}}(\eta_\star, k) &= \frac{H^2\sigma^3}{16\pi M_{\text{Pl}}^2\epsilon_{1\star}} |A_k H_\nu^{(1)}(\sigma) + B_k H_\nu^{(2)}(\sigma)|^2, \\ \mathcal{P}_{\mathcal{R}\mathcal{R}}(\eta_\star, k) &= \left(\nu - \frac{3+\epsilon_2}{2}\right) H \mathcal{P}_{\mathcal{R}\mathcal{R}}(\eta_\star, k) \\ &\quad - \frac{H^3\sigma^4}{16\pi M_{\text{Pl}}^2\epsilon_{1\star}} \left[A_k H_\nu^{(1)}(\sigma) + B_k H_\nu^{(2)}(\sigma)\right] \left[A_k^* H_{\nu-1}^{(2)}(\sigma) + B_k^* H_{\nu-1}^{(1)}(\sigma)\right],\end{aligned}\tag{3.24}$$

where $\epsilon_{1\star} = \epsilon_1(\eta_\star)$, and hence from Eq. (2.35)

$$\alpha_\star = \frac{i\sigma H}{2} \left[\frac{A_k^* H_{\nu-1}^{(2)}(\sigma) + B_k^* H_{\nu-1}^{(1)}(\sigma)}{A_k^* H_\nu^{(2)}(\sigma) + B_k^* H_\nu^{(1)}(\sigma)} \right] - \frac{i\nu H}{2}.\tag{3.25}$$

In SR and USR, $\nu = 3/2$. If we further set $(A_k, B_k) = (1, 0)$, as is the case for $\eta_t \ll \eta_\star$, one can show that this leads to

$$\alpha_\star = \frac{iH}{2} \left(\frac{\sigma^2}{1+i\sigma} - \frac{3}{2} \right).\tag{3.26}$$

To determine the initial condition for β_\star , we can perform the following conversion. The variables X in Eq. (2.18) and Y in Eq. (3.5) are related as $X = e^{\frac{1}{2}(3+\epsilon_2)Ht}Y$ and since $\pi_X = \dot{X}$ and $\pi_Y = e^{(3+\epsilon_2)Ht}\dot{Y}$, their conjugate momenta are related as $\pi_X = e^{-\frac{1}{2}(3+\epsilon_2)Ht}\pi_Y + \frac{1}{2}(3+\epsilon_2)He^{\frac{1}{2}(3+\epsilon_2)Ht}Y$. The definition of α in Eq. (2.29) can then equivalently be expressed in terms of moments of Y and π_Y as

$$\alpha = -\frac{i}{2} \frac{\langle \hat{Y} \hat{\pi}_Y \rangle}{\langle \hat{Y}^2 \rangle} e^{-(3+\epsilon_2)Ht} - \frac{i}{4}(3+\epsilon_2)H.\tag{3.27}$$

Meanwhile, since in the perturbative regime before the matching time $t < t_\star$ the wavefunction of Y is still Gaussian, $\psi_Y = (2\beta_R/\pi)^{1/4} e^{-\beta Y^2}$, one can express β in terms of the moments of Y and π_Y analogously to Eq. (2.29), i.e.

$$\beta = -\frac{i}{2} \frac{\langle \hat{Y} \hat{\pi}_Y \rangle}{\langle \hat{Y}^2 \rangle}.\tag{3.28}$$

Combining with the above expression for α , the parameters are related as

$$\beta = \left[\alpha + \frac{i}{4}(3+\epsilon_2)H \right] e^{(3+\epsilon_2)Ht},\tag{3.29}$$

and in particular at matching, using Eq. (3.26) one has¹⁵

$$\beta_\star = \frac{iH}{2} \left(\frac{\sigma^2}{1+i\sigma} + \frac{\epsilon_2}{2} \right) e^{(3+\epsilon_2)Ht_\star}.\tag{3.30}$$

¹⁵Since this is derived using Eq. (3.26), which is only valid for $\nu = 3/2$, we emphasise that this expression for β_\star is only applicable for SR ($\epsilon_2 = 0$) and USR ($\epsilon_2 = -6$).

3.3 Wigner function

We are now in a position to compute the Wigner function, introduced in Eq. (1.1). Evaluating this expression for the pure state $\hat{\rho} = |\psi\rangle\langle\psi|$, the general definition reads

$$W(\chi_0, \pi_0) = \frac{1}{2\pi} \int_{-\infty}^{\infty} du e^{-i\pi_0 u} \psi^* \left(\chi_0 - \frac{u}{2} \right) \psi \left(\chi_0 + \frac{u}{2} \right). \quad (3.31)$$

For the SR wavefunction of Eq. (3.22), this evaluates to

$$W_{\text{SR}}(\chi_0, \pi_0) = \frac{1}{\pi} \exp \left[-2\kappa^2 \beta_R \chi_0^2 - \frac{1}{2\kappa^2 \beta_R} (\pi_0 + 2\kappa^2 \beta_I \chi_0)^2 \right]. \quad (3.32)$$

We remark that this is both Gaussian and precisely of the form one would expect: In the SR case, the canonical transformation is linear, $Y = \kappa \chi_0$ and $\pi_Y = \pi_0/\kappa$, and so the functional form of the Wigner function is preserved up to coordinate transformations¹⁶ – hence why the Wigner function has the structure $\propto \exp \left[-2\beta_R Y^2 - \frac{1}{2\beta_R} (\pi_Y + 2\beta_I Y)^2 \right]$.

This will not be true of more generic non-linear transformations, as in the case of constant roll with $\epsilon_2 \neq 0$. From the form of the wavefunction in Eq. (3.21), one finds

$$W(\chi_0, \pi_0) = \frac{1}{2\pi} \left(\frac{2\kappa^2 \beta_R}{\pi} \right)^{1/2} \left(1 - e^{-2\frac{|\beta|}{\beta_R} Y_b^2} \right)^{-1} e^{-2\beta_R Y_b^2} e^{\frac{1}{2}\epsilon_2 H \chi_0} \mathcal{I}(\chi_0, \pi_0), \quad (3.33)$$

where

$$\mathcal{I} = \int_{-\infty}^{\infty} du \exp \left[-i\pi_0 u - Y_b^2 e^{\epsilon_2 H \chi_0} \left(\beta e^{\frac{1}{2}\epsilon_2 H u} + \beta^* e^{-\frac{1}{2}\epsilon_2 H u} \right) \right] \{E_1 + E_2 + E_3 + E_4\}, \quad (3.34)$$

and

$$\begin{aligned} E_1 &= \exp \left[2Y_b^2 e^{\frac{1}{2}\epsilon_2 H \chi_0} \left(\beta e^{\frac{1}{4}\epsilon_2 H u} + \beta^* e^{-\frac{1}{4}\epsilon_2 H u} \right) \right], \\ E_2 &= -\exp \left[-2Y_b^2 e^{\frac{1}{2}\epsilon_2 H \chi_0} \left(\beta e^{\frac{1}{4}\epsilon_2 H u} - \beta^* e^{-\frac{1}{4}\epsilon_2 H u} \right) \right], \\ E_3 &= -\exp \left[2Y_b^2 e^{\frac{1}{2}\epsilon_2 H \chi_0} \left(\beta e^{\frac{1}{4}\epsilon_2 H u} - \beta^* e^{-\frac{1}{4}\epsilon_2 H u} \right) \right], \\ E_4 &= \exp \left[-2Y_b^2 e^{\frac{1}{2}\epsilon_2 H \chi_0} \left(\beta e^{\frac{1}{4}\epsilon_2 H u} + \beta^* e^{-\frac{1}{4}\epsilon_2 H u} \right) \right]. \end{aligned} \quad (3.35)$$

Terms E_1 and E_4 correspond to the original and reflected Gaussian, respectively, while E_2 and E_3 represent cross terms, from which one might anticipate interference. By performing the change of variables $w = e^{\frac{1}{4}\epsilon_2 H u}$, the integral \mathcal{I} can be brought into the form

$$\mathcal{I} = \frac{4}{|\epsilon_2| H} \int_0^{\infty} dw w^{-\frac{4i\pi_0}{\epsilon_2 H} - 1} \exp \left[-Y_b^2 e^{\epsilon_2 H \chi_0} (\beta w^2 + \beta^* w^{-2}) \right] \sum_{i=1}^4 E_i, \quad (3.36)$$

with

$$\sum_{i=1}^4 E_i = 4 \sinh \left(2Y_b^2 e^{\frac{1}{2}\epsilon_2 H \chi_0} \beta w \right) \sinh \left(2Y_b^2 e^{\frac{1}{2}\epsilon_2 H \chi_0} \beta^* w^{-1} \right). \quad (3.37)$$

¹⁶The set of linear canonical transformations on phase space \mathbb{R}^2 forms the symplectic group $S_p(2, \mathbb{R})$. In quantum mechanics, these correspond to unitary operators on Hilbert space that implement the transformation of states and observables [20, 109, 110].

This integral does not have an exact closed form solution, and so must be evaluated numerically.¹⁷ We do so in the next section, where we study the behaviour of the Wigner function as the state evolves.

3.4 Comparison with linear theory

In order to verify the consistency of the above framework, let us check that standard results of cosmological perturbation theory are recovered in the linear limit. At leading order in χ_0 , the function h appearing in Eq. (3.18) is linear, namely $h_{\text{lin}}(\chi_0) = \kappa\chi_0$, hence the wavefunction of Eq. (3.21) reduces to the Gaussian form

$$\psi_{\text{lin}}(\chi_0) = \left(\frac{2\kappa^2\beta_R}{\pi} \right)^{1/4} \exp(-\kappa^2\beta\chi_0^2), \quad (3.38)$$

where we have also used Eq. (3.11) to discard terms that are exponentially suppressed by the inverse squared amplitude of the curvature perturbation. This expression coincides exactly with the SR expression of Eq. (3.22). It is then not surprising that the Wigner function for the linearised state coincides also with the SR expression (3.32),

$$W_{\text{lin}}(\chi_0, \pi_0) = \frac{1}{\pi} \exp \left[-2\kappa^2\beta_R\chi_0^2 - \frac{1}{2\kappa^2\beta_R} (\pi_0 + 2\kappa^2\beta_I\chi_0)^2 \right]. \quad (3.39)$$

One thus obtains a centred Gaussian state, with variances and covariance

$$\langle \hat{\chi}_0^2 \rangle = \frac{1}{4\kappa^2\beta_R}, \quad \langle \hat{\pi}_0^2 \rangle = \kappa^2 \frac{|\beta|^2}{\beta_R}, \quad \langle \hat{\chi}_0 \hat{\pi}_0 \rangle = \frac{i}{2} - \frac{\beta_I}{2\beta_R}, \quad (3.40)$$

where β is given in Eqs. (3.15) and (3.30). We remark that the determinant of the covariance matrix is 1/4, as one would expect for a minimum-uncertainty Gaussian state. In the late-time limit $t \rightarrow \infty$ and working to leading order in $\sigma \ll 1$, the real and imaginary parts of β have the following asymptotic behaviours for SR and USR:

$$\begin{aligned} \beta_R(t \rightarrow \infty) &= \begin{cases} \frac{1}{2}H\sigma^3 e^{3Ht_*} & (\text{SR}), \\ \frac{1}{2}H\sigma^3 e^{3H(t_*-2t)} & (\text{USR}), \end{cases} \\ \beta_I(t \rightarrow \infty) &= \begin{cases} \frac{1}{2}H\sigma^2 e^{3Ht_*} & (\text{SR}), \\ -\frac{3}{2}He^{-3Ht} & (\text{USR}). \end{cases} \end{aligned} \quad (3.41)$$

Together with the definition of κ in Eq. (3.7) and \mathcal{V} in Eqs. (2.32) and (2.33), this leads to the following late-time limits for the variances and covariance:

$$\langle \hat{\chi}_0^2 \rangle \Big|_{t \rightarrow \infty} = \begin{cases} \frac{1}{8\pi^2 M_{\text{Pl}}^2 \epsilon_{1*}} & (\text{SR}), \\ \frac{1}{8\pi^2 M_{\text{Pl}}^2 \epsilon_{1*}} \left(\frac{a}{a_*} \right)^6 & (\text{USR}), \end{cases} \quad (3.42)$$

$$\langle \hat{\pi}_0^2 \rangle \Big|_{t \rightarrow \infty} = \begin{cases} \frac{2\pi^2 M_{\text{Pl}}^2 \epsilon_{1*}}{\sigma^2} & (\text{SR}), \\ \frac{18\pi^2 M_{\text{Pl}}^2 \epsilon_{1*}}{\sigma^6} & (\text{USR}), \end{cases} \quad (3.43)$$

¹⁷It is possible to express \mathcal{I} in terms of an infinite series, which will aid in the interpretation of features in Sec. 4. We do so in Eq. (4.6).

$$\text{Re}[\langle \hat{\chi}_0 \hat{\pi}_0 \rangle] \Big|_{t \rightarrow \infty} = \begin{cases} -\frac{1}{2\sigma} & (\text{SR}), \\ \frac{3}{2\sigma^3} \left(\frac{a}{a_*}\right)^3 & (\text{USR}). \end{cases} \quad (3.44)$$

Meanwhile, in perturbation theory at leading order in gradients, the mode equation (2.36) has two homogeneous solutions

$$\mathcal{R}_{h,k} = C_k + D_k \int_{\eta_*}^{\eta} \frac{d\tilde{\eta}}{z^2(\tilde{\eta})} = C_k - \frac{D_k}{a_* z_*^2 (3 + \epsilon_2) H} \left[\left(\frac{\eta}{\eta_*} \right)^{3+\epsilon_2} - 1 \right], \quad (3.45)$$

often referred to as the “growing” and “decaying” modes, respectively. Here, the lower bound of the integral has been set to η_* for convenience, but up to a redefinition of C_k and D_k , it can be set otherwise.¹⁸ In the separate-universe approach, the homogeneous solution $\mathcal{R}_{h,k}$ is employed to describe perturbations on sufficiently large super-Hubble scales, while perturbations on smaller scales are described by the full mode function \mathcal{R}_k . To ensure consistency between the descriptions, a matching procedure is employed to set C_k and D_k such that the homogeneous solution (3.45) and the full mode function (3.23), as well as their derivatives, coincide at the matching time (see e.g. [111] for more details). This leads to the identification

$$C_k = \mathcal{R}_k(\eta_*), \quad D_k = z_*^2 \mathcal{R}'_k(\eta_*). \quad (3.46)$$

Assuming Bunch-Davies vacuum conditions $(A_k, B_k) = (1, 0)$, the super-horizon limit of the full mode function (3.23) is

$$\mathcal{R}_k(\eta) \xrightarrow{(-k\eta) \ll 1} -\frac{i 2^\nu \Gamma(\nu) \sigma^{\frac{3}{2}-\nu} H}{\sqrt{8\pi M_{\text{Pl}}^2 \epsilon_{1*} k^3}} \left(\frac{\eta}{\eta_*} \right)^{\frac{3+\epsilon_2}{2}-\nu} \left[1 + \frac{(-k\eta)^2}{4(\nu-1)} + \mathcal{O}(-k\eta)^4 \right]. \quad (3.47)$$

Recalling that $\nu = |3 + \epsilon_2|/2$, notice that the overall multiplicative factor $(\eta/\eta_*)^{\frac{3+\epsilon_2}{2}-\nu}$ vanishes for $\epsilon_2 > -3$ but not for $\epsilon_2 < -3$, such that the leading-order time dependence is $\mathcal{R}_k \sim \text{constant} + \mathcal{O}(\eta^2)$ in the former case and $\mathcal{R}_k \sim \eta^{3+\epsilon_2}$ in the latter. One can then identify the leading-order homogeneous matching coefficients (3.46) as

$$C_k = -\frac{i 2^\nu \Gamma(\nu) \sigma^{\frac{3}{2}-\nu} H}{\sqrt{8\pi M_{\text{Pl}}^2 \epsilon_{1*} k^3}}, \quad D_k = -z_*^2 C_k \begin{cases} \frac{k\sigma}{2(\nu-1)} & \epsilon_2 > -3 \\ \frac{(3+\epsilon_2)k}{\sigma} & \epsilon_2 < -3 \end{cases}, \quad (3.48)$$

where we have used that $k\eta_* = -\sigma$. From these coefficients, we construct the homogeneous mode function according to Eq. (3.45). In the late-time limit $\eta \rightarrow 0^-$ at leading order in σ , this homogeneous solution approaches

$$\mathcal{R}_{h,k}(\eta \rightarrow 0^-) = C_k \begin{cases} 1 & \epsilon_2 > -3 \\ \left(\frac{a}{a_*} \right)^{-(3+\epsilon_2)} & \epsilon_2 < -3 \end{cases}, \quad (3.49)$$

¹⁸In particular, setting the lower limit to zero and defining $\tilde{C}_k = C_k - D_k \int_0^{\eta^*} d\tilde{\eta}/z^2(\tilde{\eta})$ such that $\mathcal{R}_{h,k} = \tilde{C}_k + D_k \int_0^{\eta} d\tilde{\eta}/z^2(\tilde{\eta})$ recovers the usual intuition that at late times in a SR background, the decaying mode has decayed away such that all that remains is the constant “growing mode” solution \tilde{C}_k .

where we have also used $a = -1/H\eta$ to simplify. We can also construct the momentum conjugate to $\mathcal{R}_{h,k}$ according to $\pi_{h,k} = z^2 \mathcal{R}'_{h,k}$. Using that $z^2 = 2M_{\text{Pl}}^2 \epsilon_{1\star} a_\star^2 (a/a_\star)^{2+\epsilon_2}$, one can show that in the late-time limit it approaches

$$\pi_{h,k}(\eta \rightarrow 0^-) = -2C_k M_{\text{Pl}}^2 \epsilon_{1\star} a_\star^2 \begin{cases} \frac{k\sigma}{2(\nu-1)} & \epsilon_2 > -3, \\ \frac{(3+\epsilon_2)k}{\sigma} & \epsilon_2 < -3, \end{cases} \quad (3.50)$$

which is constant for both cases. In particular when $\nu = 3/2$ (i.e. for SR or USR), one has

$$|\mathcal{R}_{h,k}^2|_{\eta \rightarrow 0^-} = \frac{2\pi^2}{k^3} \begin{cases} \frac{H^2}{8\pi^2 M_{\text{Pl}}^2 \epsilon_{1\star}} & (\text{SR}), \\ \frac{H^2}{8\pi^2 M_{\text{Pl}}^2 \epsilon_{1\star}} \left(\frac{a}{a_\star}\right)^6 & (\text{USR}), \end{cases} \quad (3.51)$$

$$|\pi_{h,k}^2|_{\eta \rightarrow 0^-} = \frac{k^3}{2\pi^2} \begin{cases} \frac{2\pi^2 M_{\text{Pl}}^2 \epsilon_{1\star}}{\sigma^2 H^2} & (\text{SR}), \\ \frac{18\pi^2 M_{\text{Pl}}^2 \epsilon_{1\star}}{\sigma^6 H^2} & (\text{USR}), \end{cases} \quad (3.52)$$

$$(\mathcal{R}_{h,k} \pi_{h,k}^*)|_{\eta \rightarrow 0^-} = \begin{cases} -\frac{1}{2\sigma} & (\text{SR}), \\ \frac{3}{2\sigma^3} \left(\frac{a}{a_\star}\right)^3 & (\text{USR}). \end{cases} \quad (3.53)$$

Comparing with the expressions in Eqs. (3.42), (3.43), and (3.44), we see that

$$\begin{aligned} \mu_1 \mu_2 \frac{k^3}{2\pi^2} |\mathcal{R}_{h,k}^2| &= H^2 \langle \hat{\chi}_0^2 \rangle, \\ \frac{\mu_1}{\mu_2} \frac{k^3}{2\pi^2} |\pi_{h,k}^2|^2 &= \frac{\langle \hat{\pi}_0^2 \rangle}{H^2}, \\ \mu_1 \frac{k^3}{2\pi^2} (\mathcal{R}_{h,k} \pi_{h,k}^*) &= \text{Re} [\langle \hat{\chi}_0 \hat{\pi}_0 \rangle]. \end{aligned} \quad (3.54)$$

This precisely mimics the replacement rule of Eq. (2.31), which confirms that our formalism reduces to the standard separate-universe approach in the perturbative limit. In this sense, the strategy proposed in this work may be seen as a quantum version of the separate-universe, or δN , picture.

Squeezing

Before studying the Wigner function at the non-perturbative level, a word is in order regarding quantum squeezing. In the SR case, from Eqs. (3.42)-(3.44) it is clear that the covariance matrix in the plane (χ_0, π_0) freezes, and hence so does the squeezing parameter

$$r = \frac{1}{2} \cosh^{-1} (\langle \hat{\chi}_0^2 \rangle + \langle \hat{\pi}_0^2 \rangle). \quad (3.55)$$

This appears to contradict the standard lore that quantum squeezing takes place at super-Hubble scales. However, there is no real inconsistency. At leading order in the gradient expansion, and at leading order in cosmological perturbation theory, the action (2.7) does not involve χ explicitly, hence the momentum is conserved. This is reflected in the fact

that the variance $\langle \hat{\pi}_0^2 \rangle$ of Eq. (3.43) is constant, both in SR and USR. Moreover, in the presence of a dynamical attractor, the curvature perturbation is conserved at super-Hubble scales [112], which explains why $\langle \hat{\chi}_0^2 \rangle$ is conserved in the SR case – see Eq. (3.42). We thus conclude that in SR, squeezing does not occur in the (χ_0, π_0) phase-space at leading order in gradients.

There are however two caveats that are worth mentioning. First, squeezing depends on the coordinates chosen to parameterise phase-space, and hence using different canonical variables would lead to different conclusions. Squeezing is neither observable nor an intrinsic property of the quantum state for time-dependent Hamiltonians [21]. Second, the full mode function (3.23) is such that $\mathcal{R}'_k \propto a^{-1}$ at late times in SR, as can be seen from Eq. (3.47). Hence, the full conjugated momentum $\pi_{\mathcal{R},k} = z^2 \mathcal{R}'_k \propto a$ does *not* freeze, unlike the homogeneous version $\pi_{h,k}$. The reason for this can be traced back to the presence of the first gradient correction to the growing mode in Eq. (3.47) (i.e. the term in parenthesis $\propto (-k\eta)^2$), which happens to overtake the homogeneous decaying mode $\propto (-k\eta)^3$ at late times in SR. Because this gradient correction is not present in the homogeneous description, $\mathcal{R}'_{h,k} \propto a^{-2}$ and thus $\pi_{h,k} = z^2 \mathcal{R}'_{h,k} \propto \text{constant}$ in SR. The absence of squeezing in the (χ_0, π_0) plane thus reflects the fact that the separate-universe approach only keeps track of the homogeneous mode, and that squeezing in these coordinates arise from higher-gradient effects. We further discuss how these gradient corrections could be included in our formalism in Sec. 5.

Finally, note that in the USR case, for which the roles of the “growing” and “decaying” modes are switched, the mode which grows scales as $\mathcal{R}_k \propto a^3$, and hence $\pi_{\mathcal{R},k} = z^2 \mathcal{R}'_k \propto \text{constant}$ is frozen. Because the gradient correction is always subdominant, the same is true for the homogeneous description: $\mathcal{R}_{h,k} \propto a^3$ and $\pi_{h,k} \propto \text{constant}$. Consequently, for USR we expect to obtain the same squeezing in the (χ_0, π_0) plane as occurs in standard cosmological perturbation theory.

4 Results

For the sake of comparison, we begin by plotting in Fig. 1 the Wigner function in a SR background (3.32). As shown in the previous section, $W_{\text{SR}}(\chi_0, \pi_0)$ also coincides with the linear-theory result $W_{\text{lin}}(\chi_0, \pi_0)$ given in Eq. (3.39). As expected, sections of the Gaussian state trace out ellipses in phase space centred at the origin. In principle, the ellipticity is controlled by the squeezing parameter r while the orientation is determined by the squeezing angle. As discussed previously, however, there is no squeezing in the homogeneous description of the SR background since it comes from the gradient correction to the growing mode, which is absent in this description. Consequently, there is little to be gained from analysing dynamics in the homogeneous description of SR further.

4.1 Wigner oscillations and interference fringes

We now turn to the more general constant-roll Wigner function, focusing in particular on the USR case ($\epsilon_2 = -6$). In Fig. 2, we numerically evaluate Eq. (3.33) for our main

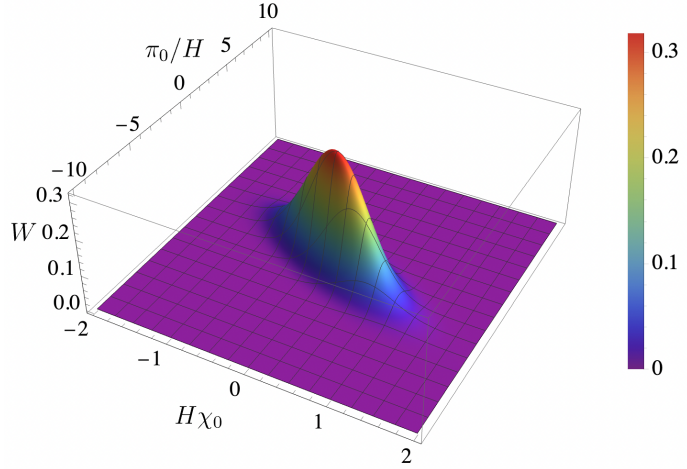


Figure 1. Wigner function in a SR background for a representative benchmark – RB in Eq. (4.1) – evaluated at $\Delta N_* \equiv N - N_* = 0$ e -folds after the matching time. Cross sections correspond to ellipses in phase space centred at the origin. Note that we plot the dimensionless combinations $H\chi_0$ and π_0/H .

reference benchmark (RB) with¹⁹

$$\text{RB: } (\bar{\mathcal{P}}_{\mathcal{R}}, \sigma) = (0.14, 1), \quad (4.1)$$

at $\Delta N_* = 0$ (left panels) and $\Delta N_* = 0.72$ (right panels), where $\Delta N_* \equiv N - N_*$ denotes the number of e -folds after the matching time. A benchmark is completely specified by just two parameters: the amplitude of curvature perturbations at the Hubble-crossing time $t = 0$, $\bar{\mathcal{P}}_{\mathcal{R}} \equiv \mathcal{P}_{\mathcal{R}\mathcal{R}}(t = 0, k) = H^2/(8\pi^2 M_{\text{Pl}}^2 \bar{\epsilon}_1)$, and the coarse graining parameter σ , which sets the matching time via $N_* = -\ln(\sigma)$. Indeed, from the expressions derived in Sec. 3, one can readily check that when χ_0 and π_0 are rescaled with H , only the two parameters above appear in the Wigner function.²⁰ The parameters are chosen such that the perturbativity condition is marginally satisfied at the matching time, hence the Wigner function already exhibits clear departures from Gaussianity at that time.²¹ Although the distribution remains relatively localised about a central peak near the origin, its previously elliptical profile has been noticeably deformed into a boomerang-shaped contour, with interference fringes extending into one quadrant. Crucially, these oscillations locally dip into negative values, so the Wigner function is no longer globally positive. The same benchmark evaluated at a later time (right panels) reveals the emergence of a cascade of rapidly oscillating interference fringes at very negative values of π_0 , far out in phase space. The envelope of these fringes appears as a repeated, mirrored replica of the central structure, while the ripples themselves exhibit decreasing amplitude and increasing oscillation frequency.

¹⁹In Appendix B.2, we demonstrate that our results are robust to modest variations in σ . The relatively large value taken here is chosen for numerical convenience.

²⁰That is, in analogy with the e -folding number $N = Ht$, we rescale the Goldstone of broken time translations as $\chi_0 \rightarrow H\chi_0$ and its conjugate momentum as $\pi_0 \rightarrow \pi_0/H$.

²¹When decreasing the value of $\bar{\mathcal{P}}_{\mathcal{R}}$, the Wigner function looks more Gaussian initially, but it then becomes numerically more difficult to track the appearance of non-Gaussian features.

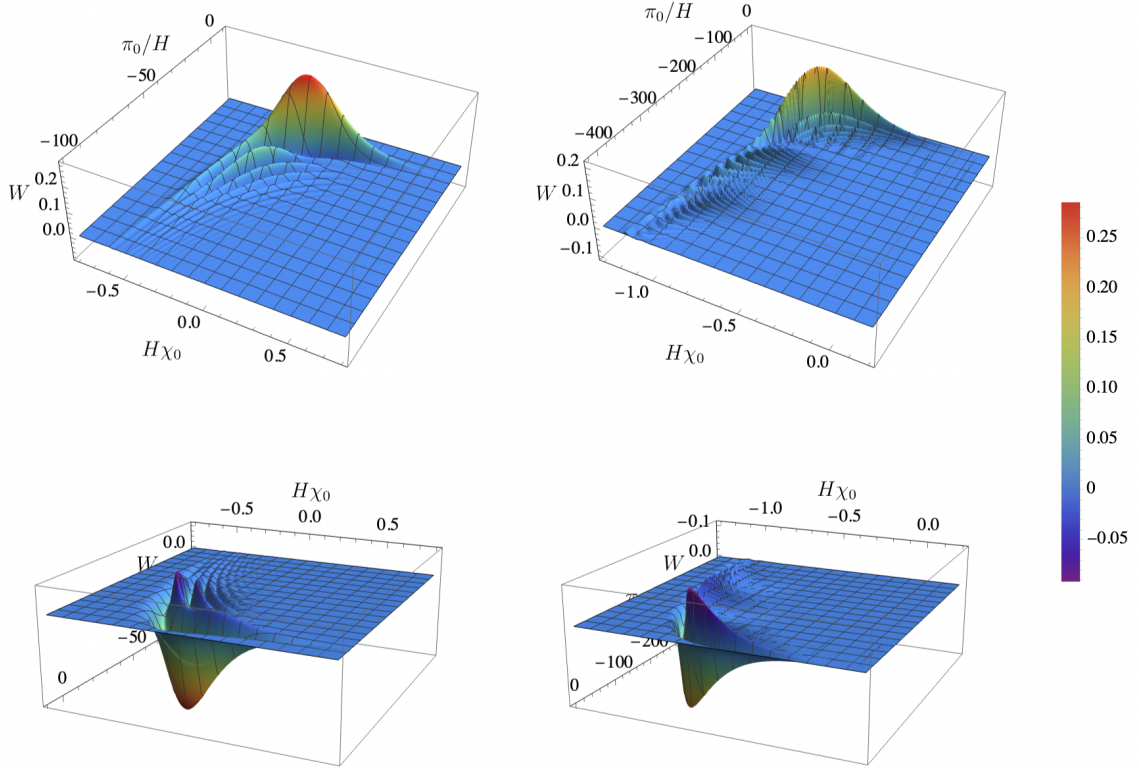


Figure 2. Wigner function in a USR ($\epsilon_2 = -6$) background for the reference benchmark in Eq. (4.1) evaluated at $\Delta N_\star = 0$ (left column) and $\Delta N_\star = 0.72$ (right column) e -folds after the matching time. The bottom panels show a different angle from which it is clear that the Wigner function assumes non-positive values.

There are in principle two sources contributing to these oscillatory features: 1) interference between the original and reflected Gaussians in (3.12), and 2) the non-linear mapping between (Y, π_Y) and the phase-space coordinates of interest (χ_0, π_0) .

Interference with the reflected Gaussian

Though each Gaussian alone would produce a strictly positive Wigner function in the (Y, π_Y) phase space, the cross terms give rise to interference in the Y -direction (and hence the χ_0 -direction after transforming back to the original variables). The nature of this interference is somewhat similar to that seen in Schrödinger cat states in quantum optics [113], which are formed from the superposition of two opposite-phase (or opposite-displacement) coherent states $|\psi_{\text{cat}}\rangle \propto (|\alpha\rangle + e^{i\theta} |-\alpha\rangle)$. The superposition of “position-space” Gaussians in (3.12) is morally similar, and upon computing²² the Wigner function corresponding to these phase-space variables $W(Y, \pi_Y)$, one observes a similar interference pattern, with an alternating series of positive and negative lobes. There is a crucial difference, however – because coherent states are defined on the full line, the interference fringes for the cat

²²We emphasise that one must compute $W(Y, \pi_Y)$ directly from $\psi_Y(Y)$, as the non-linear change of variables cannot be directly performed at the level of the Wigner function (3.33).

state are symmetric and regular. By contrast, because Y is defined on a truncated domain, the result is highly asymmetric. Further, the origin of the second term in the superposition is fundamentally different. The cat state is prepared via an external operation (one uses the annihilation operator to remove one or more photons from a squeezed vacuum state [114]) and so the two terms correspond to physical states. Whereas in our case, the reflected Gaussian feature arises to enforce the boundary condition at Y_b , namely the vanishing of the wavefunction at $\chi_0 \rightarrow \pm\infty$. In this sense, it acts analogously to an “image wavefunction” in quantum mechanics, which arises from reflection at the boundary and serves to ensure destructive interference there, rather than representing an independently prepared component of a state. After performing the change of variables back to (χ_0, π_0) , the asymmetric positive and negative lobes become additional wavelet structure on top of the envelope seen in Fig. 2. Let us finally note that the boundary condition is imposed in the asymptotic past and future, $t + \chi_0 \rightarrow \pm\infty$, which in principle requires to embed our setup in a realistic cosmological scenario. For instance, while we have considered an infinite USR phase, it is clear that it cannot extend indefinitely in the future since inflation must end at some point. How this modifies boundary conditions remains to be clarified, although we expect reflected Gaussian features to be present in general.

Non-linear mapping

While the first source of interference is present already at the level of the (Y, π_Y) variables, there is a second contribution arising from the non-linear canonical transformation (3.18) required to return to the original phase-space variables (χ_0, π_0) . That such a transformation should introduce negativity in the Wigner function is closely connected with Hudson’s theorem, which says that the only pure quantum state with a globally positive Wigner function is the Gaussian state [71]. It is thus inevitable that once the state has been re-cast in the (χ_0, π_0) variables, which renders its non-Gaussian nature manifest, local regions of negativity must appear. Unlike the contribution described above, this effect is present even in the perturbative regime, where the reflected Gaussian is irrelevant. In this sense, Wigner negativity in constant-roll backgrounds should be viewed as arising not only from non-perturbative boundary effects, but also from features present already at the perturbative level – non-perturbative methods being, however, required to monitor these features across the full phase-space region where Wigner negativity is realised, as explained in Sec. 1. In phase space, this non-linearity manifests by distorting the simple Gaussian dependence on π_Y into an infinite tower of higher harmonics in π_0 , weighted by Bessel functions whose amplitudes decay as one moves further away from the centre of the distribution.

To make this last comment more concrete, it is instructive to re-write Eq. (3.36) as follows. Using the identities [115]

$$e^{\frac{z}{2}(t+t^{-1})} = \sum_{n=-\infty}^{\infty} t^n I_n(z), \quad e^{\frac{z}{2}(t-t^{-1})} = \sum_{n=-\infty}^{\infty} t^n J_n(z), \quad (4.2)$$

where $J_n(x)$ and $I_n(x)$ are Bessel and modified Bessel functions of the first kind respectively,

one can rewrite the sum over the E_i terms as the infinite series

$$\sum_{i=1}^4 E_i = 2 \sum_{n=-\infty}^{\infty} \left(\frac{\beta}{|\beta|} \right)^{2n} \left[I_{2n} \left(4Y_b^2 |\beta| e^{\frac{1}{2}\epsilon_2 H \chi_0} \right) - J_{2n} \left(4Y_b^2 |\beta| e^{\frac{1}{2}\epsilon_2 H \chi_0} \right) \right] w^{2n}, \quad (4.3)$$

where we have used that $I_n(-z) = (-1)^n I_n(z)$ and $J_n(-z) = (-1)^n J_n(z)$. The integral appearing in (3.36) then involves terms of the form

$$\mathcal{I}_n = \int_0^\infty \frac{dw}{w} w^{-\frac{4i\pi_0}{\epsilon_2 H} + 2n} \exp \left[-Y_b^2 e^{\epsilon_2 H \chi_0} (\beta w^2 + \beta^* w^{-2}) \right], \quad (4.4)$$

which can be evaluated with the aid of the identity [115]

$$\int_0^\infty \frac{dw}{w} w^\nu e^{-aw - bw^{-1}} = 2 \left(\frac{b}{a} \right)^{\nu/2} K_\nu \left(2\sqrt{ab} \right), \quad (4.5)$$

where $K_\nu(x)$ is a modified Bessel function of the second kind. Thus, one can recast \mathcal{I} as

$$\begin{aligned} \mathcal{I}(\chi_0, \pi_0) &= \frac{8}{|\epsilon_2| H} \sum_{n=-\infty}^{\infty} \left[I_{2n} \left(4Y_b^2 |\beta| e^{\frac{1}{2}\epsilon_2 H \chi_0} \right) - J_{2n} \left(4Y_b^2 |\beta| e^{\frac{1}{2}\epsilon_2 H \chi_0} \right) \right] \\ &\quad \times \left(\frac{\beta}{|\beta|} \right)^{\frac{2i\pi_0}{\epsilon_2 H} + n} K_{-\frac{2i\pi_0}{\epsilon_2 H} + n} \left(2Y_b^2 |\beta| e^{\epsilon_2 H \chi_0} \right), \end{aligned} \quad (4.6)$$

which enters into W in Eq. (3.33). In particular, defining for conciseness $x = -\epsilon_2 H \chi_0 / 2$, $p = -2\pi_0 / \epsilon_2 H$, $\mathcal{A} = 2Y_b^2 |\beta|$, and $\beta = |\beta| e^{i\phi_\beta}$, we have

$$W(x, p) = \mathcal{M} e^{-x} \sum_{n=-\infty}^{\infty} [I_{2n}(2\mathcal{A}e^{-x}) - J_{2n}(2\mathcal{A}e^{-x})] e^{i\phi_\beta(n-ip)} K_{n+ip}(\mathcal{A}e^{-2x}), \quad (4.7)$$

with

$$\mathcal{M} = \frac{1}{2\pi} \frac{8}{|\epsilon_2|} \left(\frac{2\kappa^2 \beta_R}{\pi} \right)^{1/2} \left(1 - e^{-2\frac{|\beta|^2}{\beta_R} Y_b^2} \right)^{-1} e^{-2\beta_R Y_b^2}. \quad (4.8)$$

Writing the Wigner function in this form offers not just a practical advantage, since in practice only a finite number²³ of terms about $n = 0$ need be kept in order to faithfully capture the result of a full numerical evaluation, but it also offers conceptual clarity. Since $I_{2n}(z) - J_{2n}(z) \geq 0$ for real, non-negative argument $z \in \mathbb{R}_{\geq 0}$ and $n \in \mathbb{Z}$, this term cannot generate negativity. The exponential factor²⁴ $e^{i\phi_\beta(n-ip)} = e^{in\phi_\beta} e^{\phi_\beta p}$ contains a real, strictly positive dependence on the phase-space variable p through $e^{\phi_\beta p}$, and therefore cannot induce oscillations or negativity. The complex phase $e^{in\phi_\beta}$ can generate interference through the sum over n , but since it is independent of the phase-space variables, it does not induce oscillatory or sign-changing dependence on x or p . Dynamically, oscillations and

²³When truncating the sum at finite n , care must be taken to include both the positive and negative terms in each $\pm n$ pair so that the result is real, as required for the Wigner function.

²⁴This $e^{\phi_\beta p}$ factor is the origin of the asymmetry between positive and negative values of $\pi_0 \propto p$. Since $\phi_\beta < 0$ is negative, as can be seen from (3.15), large positive values of $\pi_0 \propto p$ are exponentially suppressed, whereas negative values are not.

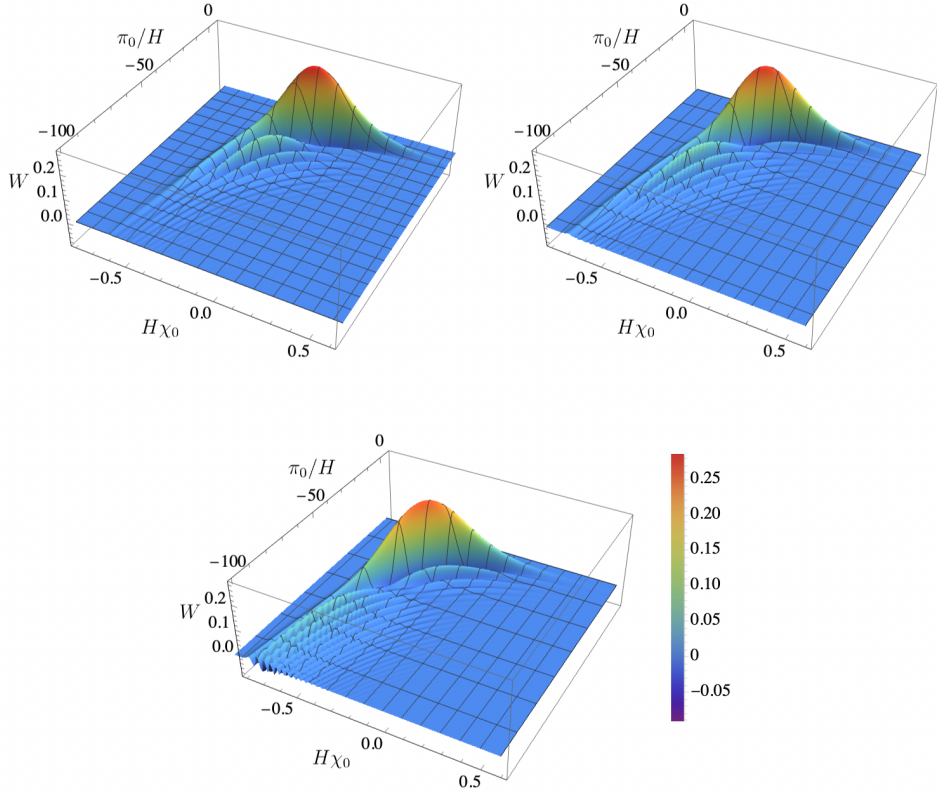


Figure 3. USR Wigner function evaluated at three sample time steps: $\Delta N_\star = 0$ (top left), $\Delta N_\star = 0.17$ (top right), and $\Delta N_\star = 0.35$ (bottom), where $\Delta N_\star = N - N_\star$ is the number of e -folds after the matching time. Note that at later times, the full distribution extends beyond the small inset shown here (see Fig. 2). Other parameters fixed to RB values – see Eq. (4.1). A video of the time evolution is available [via this link](#).

negativity can arise *only* through $K_{n+ip}(z)$. The modified Bessel function of the second kind with complex index ν is generically oscillatory provided $\text{Im}[\nu] \neq 0$, and the zeroes have been studied in e.g. [116], which provides analytic formulae in the limits $|\nu| \ll 1$ and $|\nu| \gg 1$. Unfortunately these are not particularly useful here, however; while the largest contribution to the infinite sum typically comes from $n = 0$, the first few non-zero terms $n = \pm 1, 2, 3 \dots$ can also contribute appreciably. Thus, the locations of the zeroes are the result of a complex interplay between the different contributions of $K_{n+ip}(z)$ and their weighting factors.

Nevertheless, a few general statements can be made. In the limit $|\nu| \gg 1 \gg |z|$, the zeroes of $K_\nu(z)$ are roughly exponentially spaced, $z_\ell \sim \nu \exp[-i\pi(\ell - 1/4)/\nu]$, and clustered about $z \sim 0$ [116]. Since in our case $z \sim e^{-2x}$, at large $|p|$ they should appear roughly linear in x and be clustered about small values $|x| \lesssim 1$, which is indeed seen in Fig. 2. Additionally, at fixed n , the amplitude of oscillations becomes smaller and the frequency becomes larger, respectively, for larger values of $|\text{Im}[\nu]| = |p|$. This too is reflected in Fig. 2, as the interference fringes become smaller in amplitude but larger in frequency as

one moves outwards in phase space to larger values of $|p|$. Finally, we remark that in order for the representation (4.7) with a truncated sum to faithfully capture the behaviour of W at larger values of $|\pi_0| \propto |p|$, one must retain an increasing number of terms in the sum over n . In particular, while the low- n terms are sufficient to resolve the smooth pseudo-Gaussian shape near the origin, higher- n terms are required in order to resolve the high-frequency oscillations at large $|\pi_0|$. This is consistent with the interpretation that the non-linear canonical transformation maps a simple Gaussian dependence in the variables (Y, π_Y) into an infinite tower of harmonics in π_0 , with higher harmonics progressively activated only at larger momenta.

The form of the Wigner function in Eq. (4.7) also allows us to make sense of the evolution of W with increasing time, as shown in Figs. 2 and 3. As time progresses, the distribution becomes less sharply localised about the origin and stretches in the π_0 direction, reflecting the squeezing discussed at the end of Sec. 3.4. At later times, additional ripples appear at large, negative values of π_0 . This behaviour can be understood from Eqs. (3.15) and (4.7) – with time, the argument of the modified Bessel function $\propto |\beta(t)|$ decreases. In this regime, $K_\nu(z \ll 1)$ features higher-frequency, smaller-amplitude oscillations. The new zeroes correspond to higher values of n in the sum, which are most strongly supported when $|p| \sim |n|$. Additionally, ϕ_β becomes more negative with advancing time; the factor $e^{\phi_\beta p}$ then suppresses positive values and enhances negative values of the conjugate momentum, effectively pushing the oscillatory structure outwards in $\pi_0 \propto p$.

4.2 Wigner negativity

In order to quantitatively study how the negativity of $W(\chi_0, \pi_0)$ evolves with time, we evaluate the Wigner negativity volume introduced in Eq. (1.6). This quantity vanishes for states with positive Wigner functions, while more generally $\mathcal{N} > 0$. The magnitude of \mathcal{N} quantifies the quantum interference encoded in $W(\chi_0, \pi_0)$, with larger values corresponding to more dramatically non-classical states. Conversely, a suppressed \mathcal{N} signals the emergence of an effectively classical phase-space distribution. In Fig. 4 we plot the negativity volume as a function of time, parameterized by the number of e -foldings $N = Ht$ since the matching time N_* , i.e. $\Delta N_* \equiv N - N_*$, for our representative benchmark RB in (4.1) as well as for a second benchmark with a slightly larger curvature perturbation amplitude at Hubble crossing.

The first thing to note is that \mathcal{N} grows monotonically with time. The growth law is in principle inherited from the time evolution of $\beta(t)$; however, because β enters the Wigner function W in a highly non-linear manner, and because \mathcal{N} itself depends non-linearly on W , an analytic derivation of this relationship is not feasible. Instead, fitting the numerically evaluated $\mathcal{N}(\Delta N_*)$ reveals that, at early times, the growth is well-described by the exponential form

$$\mathcal{N}(\Delta N_*) = c_1 e^{2\Delta N_*} + c_2, \quad (4.9)$$

where the fitting coefficients (c_1, c_2) depend on the benchmark under consideration and must be determined empirically. It is rather suggestive that the negativity initially appears to grow as $e^{2\Delta N_*} \propto a^2$. Whether this behaviour persists to later times remains unclear,

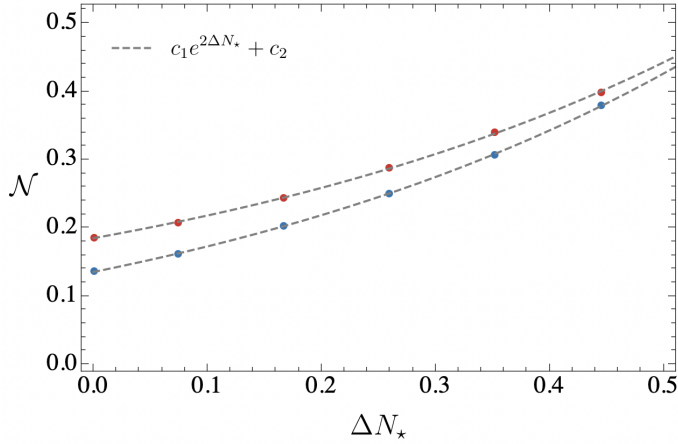


Figure 4. Wigner negativity \mathcal{N} of Eq. (1.6) as a function of the number of e -folds since matching, $\Delta N_\star = N - N_\star$, for our reference benchmark of Eq. (4.1) (red) and a second benchmark with a larger scalar amplitude $(\bar{\mathcal{P}}_{\mathcal{R}}, \sigma) = (0.28, 1)$ (blue). The negativity evolution is well-fit by an exponential growth law $\mathcal{N} = c_1 e^{2\Delta N_\star} + c_2$. For the reference benchmark, the fitting coefficients are empirically found to be $(c_1, c_2) = (0.15, 0.035)$; for the second benchmark, $(c_1, c_2) = (0.17, -0.034)$.

as numerical methods become difficult to implement efficiently once the function becomes highly oscillatory and squeezing necessitates a denser grid. Nevertheless, the observed growth is clearly convex upwards and shows no indication of saturation over the range readily accessible to our analysis.

One may be surprised that, in Fig. 4, larger values for $\bar{\mathcal{P}}_{\mathcal{R}}$ result in smaller negativity: since $\bar{\mathcal{P}}_{\mathcal{R}}$ sets the amplitude of curvature perturbations at Hubble crossing, it also governs the magnitude of non-perturbative effects and, one might therefore expect, the negativity itself. There are however two reasons that explain this seemingly counter-intuitive behaviour. First, extrapolating the empirical growth law in Eq. (4.9) to late times reveals that the negativity associated with larger $\bar{\mathcal{P}}_{\mathcal{R}}$ eventually overtakes that of our reference benchmark. Second, it is important to emphasise the there exists both a perturbative region of phase space ($|\epsilon_2 H \chi_0| < 1$) and a non-perturbative one. As $\bar{\mathcal{P}}_{\mathcal{R}}$ decreases, the support of the Wigner function becomes increasingly concentrated in the perturbative region, although it continues to extend over both regions. We have explicitly verified that, when the negativity is computed by restricting to the perturbative region only, smaller values of $\bar{\mathcal{P}}_{\mathcal{R}}$ indeed lead to smaller negativity, in agreement with expectations. See Fig. 6 in Appendix B.1.

4.3 Parametric exploration

One can also study how the Wigner function changes upon varying the other parameters thus far held fixed. Fig. 5 shows the USR Wigner function for two sample values of $\bar{\mathcal{P}}_{\mathcal{R}}$. The left panel corresponds to the RB value (4.1), while the right panel shows a value smaller by a factor of 10. For the smaller value, the central boomerang-shaped contour becomes more symmetrically rounded, with additional wavelet structure on top of the envelope seen in the left panel. This behaviour can be understood from the form of Eq. (4.7) and the fact that

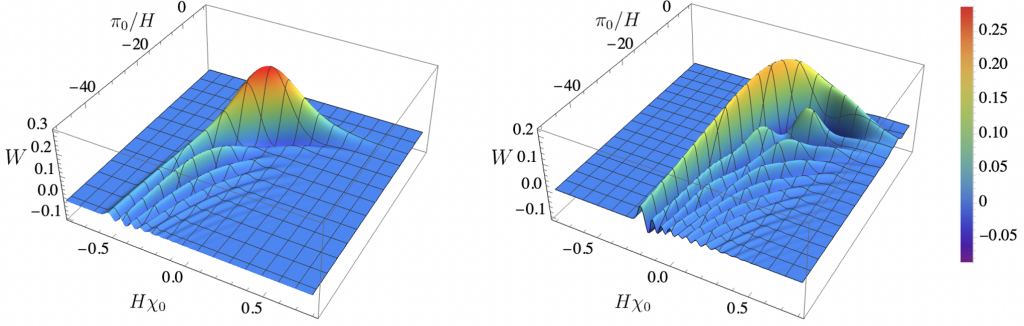


Figure 5. Left: USR Wigner function for RB values, $(\bar{P}_R, \sigma) = (0.14, 1)$, at $\Delta N_\star = 0$. **Right:** Same plot for $(\bar{P}_R, \sigma) = (0.014, 1)$, also evaluated at $\Delta N_\star = 0$.

$M_{\text{Pl}}^2 \epsilon_{1*}/H^2 \propto \mathcal{A}$ appears in the argument of the Bessel functions $I_{2n}(2\mathcal{A}e^{-x})$, $J_{2n}(2\mathcal{A}e^{-x})$, and $K_{n+ip}(\mathcal{A}e^{-2x})$. Increasing \mathcal{A} modifies the balance between these functions, enhancing interference among nearby modes in the series to give rise to the nested wavelet modulations on top of the existing envelope. Further, this larger \mathcal{A} forces the oscillations, which appear for small argument of the modified Bessel $K_{n+ip}(\mathcal{A}e^{-2x})$, to cluster more closely about $x \propto \chi_0 \sim 0$, as can be seen in the right panel.

Finally, one can also vary the coarse-graining parameter σ , which controls the scale at which modes are transferred from the short-wavelength sector to long-wavelength effective theory. In our convention, $N_\star = -\ln(\sigma)$, and so decreasing σ corresponds to performing the matching at a later time. In the separate-universe approach, physical observables are expected to be independent of the choice of σ , provided it is taken to be sufficiently small. This is true at the perturbative level; in the present framework, mild σ -dependence is expected since non-linearities are only included after the matching time. Consequently, taking σ to be too small decreases the interval for which non-linear effects are incorporated and therefore underestimates their impact. We have verified that our results are otherwise robust to moderate variations in σ (see Fig. 7 in Appendix B.2).

5 Discussion

These results have a number of implications. Perhaps the most glaring is that quantum effects *can* become important, potentially even preventing a stochastic description, for inflationary backgrounds that deviate from slow-roll evolution and develop large fluctuations. Recall that a necessary, though not sufficient, condition for formulating a stochastic description in terms of the Wigner function is that this object be everywhere positive, such that its probabilities are meaningful. This condition fails in certain regions of parameter space, as can be seen in the figures of Sec. 4. The Wigner negativity can be quite sizeable and generically increases with time (see Fig. 4). Consequently, W cannot be interpreted as a true probability distribution. It is worth remarking that since W is still positive over certain regions of parameter space, one may still be able to use a stochastic description to reproduce with good accuracy some observables provided their support in phase space co-

incides with these positive regions. This is probably the case if the amplitude of curvature perturbations remains small and one is interested in measuring low-order correlation functions. However, that the negative regions appear already quite close to the origin in phase space for the USR models studied here bodes well for identifying an observable involving large-density objects (such as ultra-compact dark matter halos or primordial black holes) sensitive to this Wigner negativity, which we leave to future work.

This finding runs contrary to the standard lore, which holds that the squeezing that occurs while modes are outside the Hubble radius is responsible for their “classicalisation”. Instead, we find that the squeezing picture – or equivalently, the hierarchy of linear-theory growing and decaying modes – is insufficient to diagnose classicality. In retrospect, this should not be too surprising. As we have already remarked, the success of a stochastic description in reproducing the most relevant observables (e.g. 2-point functions of Hermitian observables) is actually attributable to working in the linear theory [12], which preserves a Gaussian state. A squeezed state is still a very quantum state, as is appreciated in quantum optics and other fields; it just appears classical for a certain class of coarse-grained observables. Further, because the squeezing amplitude can always be changed (or even eliminated) by an appropriate canonical transformation, there is no reason why it should be a meaningful reflection of the intrinsic properties of the state [21].

Another important lesson to take away is that slow-roll and ultra-slow-roll backgrounds have surprising qualitative differences. Again, if one follows the schematic squeezing argument, one would reason that slow roll and ultra-slow roll should be equally classical, since even though what is called the growing and decaying mode switches between the cases, in both backgrounds one mode dominates over the other. We see that this is not so. One may have also expected a certain symmetry between the slow-roll and ultra-slow-roll results on the basis of the Wands duality [105], which relates the spectra of perturbations in cosmological backgrounds with the same Mukhanov-Sasaki mass term z''/z , which can be expressed exactly in terms of Hubble-flow parameters as

$$\frac{z''}{z} = \mathcal{H}^2 \left(2 - \epsilon_1 + \frac{3}{2} \epsilon_2 - \frac{1}{2} \epsilon_1 \epsilon_2 + \frac{1}{4} \epsilon_2^2 + \frac{1}{2} \epsilon_2 \epsilon_3 \right). \quad (5.1)$$

Because for both slow-roll ($\epsilon_1, \epsilon_2, \epsilon_3 \ll 1$) and ultra-slow-roll ($\epsilon_1, \epsilon_3 \ll 1, \epsilon_2 \simeq -6$) backgrounds one has $z''/z \simeq 2\mathcal{H}^2$, linear perturbations in these backgrounds have identical spectra when expressed in terms of the Mukhanov-Sasaki variable $v_k = z\mathcal{R}_k$. While one does see avatars of this duality in the intermediate steps of the calculation performed above,²⁵ it does not survive the non-linear mapping.

Finally, perhaps the most significant implication of the above results is that the prospect of detecting a genuinely quantum signature of our universe’s origins in cosmological observables may be less bleak than previously thought. There is, in principle, a substantial degree of “quantumness” encoded in the CMB. As discussed in Sec. 1, one manifestation of this is the substantial amount of quantum entanglement between opposite Fourier modes, which nevertheless does not lead to significant quantum correlations in real

²⁵For example, the potential $V(X)$ of Eq. (3.3) and the Bessel index $\nu = |3 + \epsilon_2|/2$ for the mode functions in Eq. (3.23) are identical for SR ($\epsilon_2 = 0$) and USR ($\epsilon_2 = -6$) backgrounds.

space. The appearance of regions of negativity in the Wigner function instead suggests that there should exist observables sensitive to the quantum interferences present in non-slow-roll backgrounds. Determining what these observables are should be a major programme going forward.

There are several natural directions along which the present work can be extended. To place them in context, it is useful to situate our approach within the landscape of δN -based methods, which are all rooted in the separate-universe picture discussed in Sec. 2.4. Within this landscape, one may broadly distinguish between the original δN formalism, which describes a classical closed system, and its stochastic generalisation, which remains classical but treats the long-wavelength sector as an open system by coarse-graining at a fixed physical scale and incorporating backreaction from short-wavelength modes as they join the system. The framework developed here can be viewed as a quantum version of the separate-universe picture underlying the δN formalism, since we work at fixed comoving scale within a closed, but fully quantum, system. This perspective immediately suggests two extensions:

- **Gradient corrections:** The separate-universe approach corresponds to the lowest-order approximation in a gradient expansion and therefore breaks down when these gradient terms become important, such as during sudden transitions away from the slow-roll attractor [117]. Deviations from slow-roll behaviour are necessary in single-field models seeking to enhance small-scale power, a scenario of much theoretical interest and one in which genuinely quantum effects, such as interferences in the Wigner function, are expected to play a significant role. In this work, we have focused on the USR phase, but the inclusion of gradient corrections would enable the embedding of this USR phase in a realistic scenario that includes transitions from, and to, the SR attractor. Extensions of the classical and stochastic δN formalisms incorporating gradient corrections have recently been explored in [111, 118, 119]. Developing an analogous extension within our fully quantum framework would be a natural next step.
- **Open-system effects:** Our analysis has thus far treated the system as closed and neglected environmental decoherence, which is expected to play an important role in the classicalisation of inflationary perturbations. A more realistic treatment should instead model the system as open, either through stochastic effects²⁶ associated with modes crossing into the system, or through coupling to an external bath representing other environmental degrees of freedom, such as entropic perturbations. One avenue towards investigating these effects without committing to a specific microphysical realisation of the environment is the open EFT of inflation [120], which extends the EFT framework to incorporate dissipation, noise, and decoherence. The master equations for the density matrix that these open theories provide can be unravelled into stochastic Schrödinger equations [121], and computing the Wigner function along

²⁶This can be accomplished by coarse graining at a fixed physical – rather than comoving – scale.

their realisations should allow one to monitor environmental effects on quantum interferences.

Understanding how such effects modify the Wigner negativity observed here remains an important open question. Nevertheless, the fact that such pronounced negativity occurs already in one of the simplest well-motivated non-slow-roll backgrounds is very encouraging. Further, that this negativity occurs so close to the origin in phase space when cosmological fluctuations are large suggests that the associated quantum interference effects may be accessible to cosmological observables involving large-density objects such as ultra-compact halos or primordial black holes. Our results demonstrate that going beyond linear order and slow-roll evolution opens up a qualitatively new regime in which the quantum nature of primordial fluctuations may manifest. Moreover, the framework developed here provides an ideal theoretical setting in which these and further questions can be systematically explored.

Acknowledgments

The authors would like to thank G. Barenboim, H. Firouzjahi, D. Kaiser, and B. Nikbakht for useful conversations. AI would also like to thank M. Von Drasek for providing computational resources. AI is supported by NSF Grant PHY-2310429, Simons Investigator Award No. 824870, DOE HEP QuantISED award #100495, the Gordon and Betty Moore Foundation Grant GBMF7946, and the U.S. Department of Energy (DOE), Office of Science, National Quantum Information Science Research Centers, Superconducting Quantum Materials and Systems Center (SQMS) under contract No. DEAC02-07CH11359. Some of the computing for this project was performed on the Sherlock cluster. The authors would like to thank Stanford University and the Stanford Research Computing for providing computational resources and support that contributed to these research results.

A Canonical transformations and boundary terms

Here we demonstrate how one may remove total time derivative terms in the action by making appropriate canonical transformations. We first review the formalism developed in [20, 122, 123] to determine new phase-space variables which simplify a Hamiltonian system. Then, as an example, we demonstrate how to use this formalism to eliminate the total time derivative in Eq. (2.6).

A.1 Canonical transformations

Consider the field $\chi(t, \mathbf{x})$ and its conjugate momentum $\pi_\chi(t, \mathbf{x})$ which satisfy the following Poisson bracket

$$\{\chi(t, \mathbf{x}), \pi_\chi(t, \mathbf{y})\} = \delta^{(3)}(\mathbf{x} - \mathbf{y}), \quad (\text{A.1})$$

for all t . The Hamiltonian density $\mathsf{H}(\chi, \pi_\chi, t)$ governs the dynamics of the system by defining the equations of motion

$$\dot{\chi} = \frac{\partial \mathsf{H}}{\partial \pi_\chi}, \quad \dot{\pi}_\chi = -\frac{\partial \mathsf{H}}{\partial \chi}. \quad (\text{A.2})$$

A canonical transformation is a transformation of phase-space variables which preserves the Poisson bracket. That is, we define new canonical variables $\tilde{\chi}, \tilde{\pi}_\chi$ which obey the same Poisson bracket structure

$$\{\tilde{\chi}(t, \mathbf{x}), \tilde{\pi}_\chi(t, \mathbf{y})\} = \delta^{(3)}(\mathbf{x} - \mathbf{y}). \quad (\text{A.3})$$

The new Hamiltonian density $\tilde{\mathsf{H}}$ determines the evolution of the new variables via

$$\dot{\tilde{\chi}} = \frac{\partial \tilde{\mathsf{H}}}{\partial \tilde{\pi}_\chi}, \quad \dot{\tilde{\pi}}_\chi = -\frac{\partial \tilde{\mathsf{H}}}{\partial \tilde{\chi}}. \quad (\text{A.4})$$

In practice, one can find the new Hamiltonian density $\tilde{\mathsf{H}}$ with the aid of the generating function \mathcal{F}_i . There are four types of generating function, corresponding to the four possible types of canonical transformations. We will focus on the Type II transformation with generating function $\mathcal{F}_2 = \mathcal{F}_2(\chi, \tilde{\pi}, t)$, since this will be the type required to eliminate the boundary terms in both Eq. (2.6) and Eq. (2.24). In Type II transformations, the original momentum π_χ and new canonical variable $\tilde{\chi}$ are expressed in terms of the new momentum $\tilde{\pi}_\chi$ and original variable χ and determined by the generating function as

$$\pi_\chi = \frac{\partial \mathcal{F}_2}{\partial \chi}, \quad \tilde{\chi} = \frac{\partial \mathcal{F}_2}{\partial \tilde{\pi}_\chi}. \quad (\text{A.5})$$

The new Hamiltonian density is found by demanding that the least action principle derived from the action corresponding to the original Hamiltonian remain invariant under the canonical transformation. This leads to

$$\tilde{\mathsf{H}}(\tilde{\chi}, \tilde{\pi}_\chi) = \mathsf{H}(\chi(\tilde{\chi}, \tilde{\pi}_\chi), \pi_\chi(\tilde{\chi}, \tilde{\pi}_\chi)) + \frac{\partial \mathcal{F}_2}{\partial t} \Big|_{\chi(\tilde{\chi}, \tilde{\pi}_\chi), \tilde{\pi}_\chi}. \quad (\text{A.6})$$

A.2 Example: simplifying Eq. (2.6)

As an example, we demonstrate how to eliminate the total-derivative term in Eq. (2.6), which corresponds to the Lagrangian

$$\mathcal{L} = M_{\text{Pl}}^2 a^3(t) H^2(t) \epsilon_1(t + \chi) \left[\dot{\chi}^2 - \frac{1}{a^2(t)} (\partial \chi)^2 \right] - \frac{d}{dt} \left[2M_{\text{Pl}}^2 a^3(t) H(t + \chi) \right], \quad (\text{A.7})$$

where, hereafter, the contributions from the total-derivative term are displayed in blue. The momentum conjugate to χ is defined as $\pi_\chi = \frac{\partial \mathcal{L}}{\partial \dot{\chi}}$, leading to

$$\pi_\chi = 2M_{\text{Pl}}^2 a^3(t) H^2(t) \epsilon_1(t + \chi) (1 + \dot{\chi}), \quad (\text{A.8})$$

where we recall that in the decoupling limit we work at leading order in ϵ_1 . The Hamiltonian can then be obtained by the Legendre transform $\mathsf{H} = \pi_\chi \dot{\chi} - \mathcal{L}$,

$$\begin{aligned} \mathsf{H} = & \frac{\pi_\chi^2}{4M_{\text{Pl}}^2 a^3(t) H^2(t) \epsilon_1(t + \chi)} + M_{\text{Pl}}^2 a(t) H^2(t) \epsilon_1(t + \chi) (\partial \chi)^2 \\ & - M_{\text{Pl}}^2 a^3(t) H^2(t) \epsilon_1(t + \chi) - \pi_\chi + 6M_{\text{Pl}}^2 a^3(t) H(t) H(t + \chi). \end{aligned} \quad (\text{A.9})$$

Since the Hamiltonian is quadratic in π_χ but highly non-linear in χ , let us look for a canonical transformation where only the momentum is redefined. In addition, since χ and t only appear through the combinations t and $t + \chi$ in the Hamiltonian, let us consider a canonical transformation of the form

$$\chi = \tilde{\chi}, \quad \pi_\chi = \tilde{\pi}_\chi + \textcolor{magenta}{h(t)g(t + \tilde{\chi})}. \quad (\text{A.10})$$

Hereafter, we display in magenta the terms arising from the canonical transformation. From Eq. (A.5), such a transformation follows from the Type II generating function

$$\mathcal{F}_2(\chi, \tilde{\pi}_\chi, t) = \chi \tilde{\pi}_\chi + \textcolor{magenta}{h(t)G(t + \chi)}, \quad (\text{A.11})$$

where $\partial_\chi G = g$. Making use of Eq. (A.6), the new Hamiltonian density reads

$$\begin{aligned} \tilde{H} = & \frac{\tilde{\pi}_\chi^2}{4M_{\text{Pl}}^2 a^3(t) H^2(t) \epsilon_1(t + \tilde{\chi})} + M_{\text{Pl}}^2 a(t) H^2(t) \epsilon_1(t + \tilde{\chi}) (\partial \tilde{\chi})^2 \\ & + \tilde{\pi}_\chi \left[\frac{\textcolor{magenta}{h(t)g(t + \tilde{\chi})}}{2M_{\text{Pl}}^2 a^3(t) H^2(t) \epsilon_1(t + \tilde{\chi})} - \textcolor{blue}{1} \right] \\ & + M_{\text{Pl}}^2 a^3(t) H^2(t) \epsilon_1(t + \tilde{\chi}) \left\{ \left[\frac{\textcolor{magenta}{h(t)g(t + \tilde{\chi})}}{2M_{\text{Pl}}^2 a^3(t) H^2(t) \epsilon_1(t + \tilde{\chi})} \right]^2 - \textcolor{blue}{1} \right\} \\ & + \textcolor{blue}{6M_{\text{Pl}}^2 a^3(t) H(t) H(t + \tilde{\chi})} + \textcolor{magenta}{\dot{h}(t)G(t + \tilde{\chi})}. \end{aligned} \quad (\text{A.12})$$

From the above expression, it is clear that the functions h and g that allow the terms generated by the canonical transformation to cancel out those coming from the total derivative are $h(t) = 2M_{\text{Pl}}^2 a^3(t) H^2(t)$ and $g(t + \tilde{\chi}) = \epsilon_1(t + \tilde{\chi})$, for which $G(t + \tilde{\chi}) = -H(t + \tilde{\chi})/H^2(t)$. We therefore conclude that, under the redefinition

$$\chi = \tilde{\chi}, \quad \pi_\chi = \tilde{\pi}_\chi + 2M_{\text{Pl}}^2 a^3(t) H^2(t) \epsilon_1(t + \tilde{\chi}), \quad (\text{A.13})$$

the Hamiltonian reduces to the first line in Eq. (A.12), which is the expression used in the main text.

B Additional plots

B.1 Negativity within the perturbative domain

In Fig. 6 we restrict the computation of Wigner negativity to the phase-space region $|\epsilon_2 H \chi_0| < 1$ corresponding to curvature perturbations being indeed perturbative. Note that, since the action (2.7) is quadratic in $\dot{\chi}$ but highly non-linear in χ , perturbativity, defined as the phase-space domain which can be properly described by the action when truncated at second order in χ and $\dot{\chi}$, only involves an upper bound on $|\chi|$. Negativity increases with $\bar{\mathcal{P}}_{\mathcal{R}}$, in agreement with the intuition that larger $\bar{\mathcal{P}}_{\mathcal{R}}$ results in stronger non-perturbative effects, and hence larger negativity.

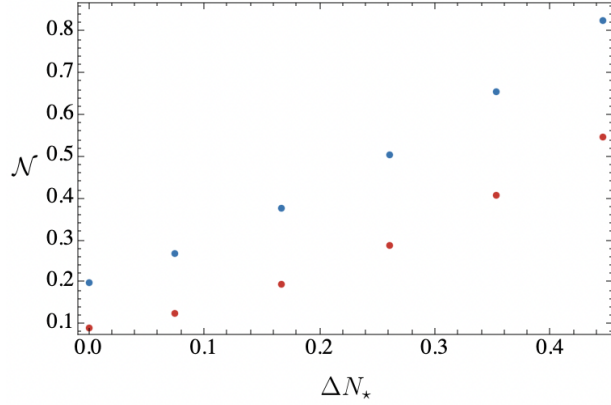


Figure 6. Wigner negativity (4) for the reference benchmark of Eq. (4.1) (red) and a second benchmark with $(\bar{\mathcal{P}}_{\mathcal{R}}, \sigma) = (0.28, 1)$ computed by restricting the integration domain to the perturbative regime ($|\epsilon_2 H \chi_0| < 1$). Comparing this behaviour with Fig. 4, one sees that the trend has flipped, such that smaller scalar amplitude values $\mathcal{P}_{\mathcal{R}}$ are associated with smaller negativities.

B.2 Varying the coarse-graining parameter

Here we check that our results are relatively robust under modest variations in the coarse-graining parameter σ . As illustrated in Fig. 7 for two representative benchmarks, the

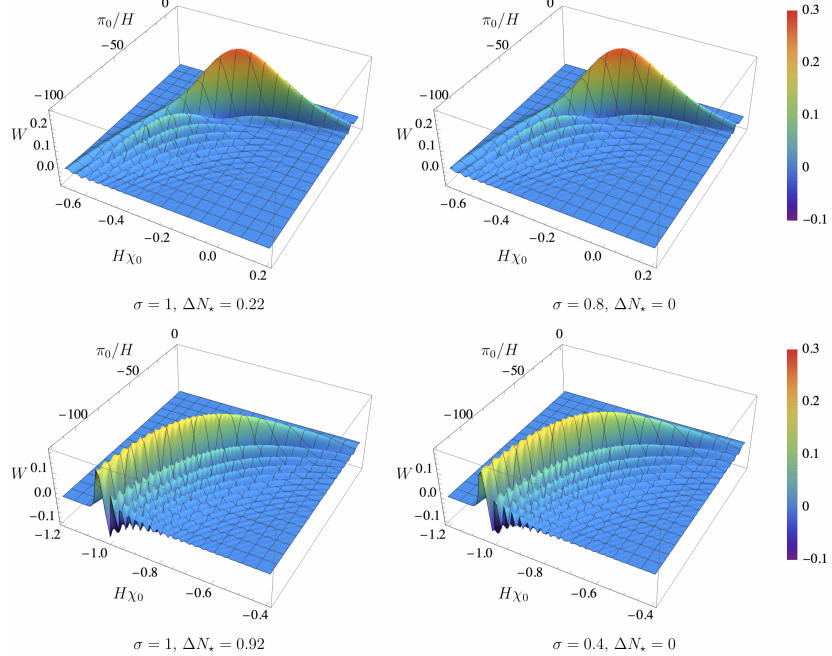


Figure 7. USR Wigner function upon varying the coarse-graining parameter σ . **Top:** W for $\sigma = 1$ and $\Delta N_★ = -\ln(0.8)$ (left) compared with $\sigma = 0.8$ and $\Delta N_★ = 0$ (right). **Bottom:** W for $\sigma = 1$ and $\Delta N_★ = -\ln(0.4)$ (left) compared with $\sigma = 0.4$ and $\Delta N_★ = 0$ (right). All panels are evaluated at the same time N and $\bar{\mathcal{P}}_{\mathcal{R}}$ is set to the RB value (4.1).

differences are visually imperceptible. This behaviour is expected to persist for modestly smaller values of σ , although demonstrating this would require impractically dense sampling. The tiny residual discrepancies between the left and right panels arise because, in our separate-universe-inspired framework, non-linear effects are included only *after* the matching time $N_\star = -\ln(\sigma)$. Consequently, taking σ to be too small leads to an underestimation of their impact.

References

- [1] A.A. Starobinsky, *A New Type of Isotropic Cosmological Models Without Singularity*, *Phys. Lett. B* **91** (1980) 99.
- [2] K. Sato, *First-order phase transition of a vacuum and the expansion of the Universe*, *mnras* **195** (1981) 467.
- [3] A.H. Guth, *The Inflationary Universe: A Possible Solution to the Horizon and Flatness Problems*, *Phys. Rev. D* **23** (1981) 347.
- [4] A.D. Linde, *A New Inflationary Universe Scenario: A Possible Solution of the Horizon, Flatness, Homogeneity, Isotropy and Primordial Monopole Problems*, *Phys. Lett. B* **108** (1982) 389.
- [5] A. Albrecht and P.J. Steinhardt, *Cosmology for Grand Unified Theories with Radiatively Induced Symmetry Breaking*, *Phys. Rev. Lett.* **48** (1982) 1220.
- [6] A.A. Starobinsky, *Spectrum of relict gravitational radiation and the early state of the universe*, *JETP Lett.* **30** (1979) 682.
- [7] V.F. Mukhanov and G.V. Chibisov, *Quantum Fluctuations and a Nonsingular Universe*, *JETP Lett.* **33** (1981) 532.
- [8] A.H. Guth and S.Y. Pi, *Fluctuations in the New Inflationary Universe*, *Phys. Rev. Lett.* **49** (1982) 1110.
- [9] A.A. Starobinsky, *Dynamics of Phase Transition in the New Inflationary Universe Scenario and Generation of Perturbations*, *Phys. Lett. B* **117** (1982) 175.
- [10] J.M. Bardeen, P.J. Steinhardt and M.S. Turner, *Spontaneous creation of almost scale-free density perturbations in an inflationary universe*, *prd* **28** (1983) 679.
- [11] PLANCK collaboration, *Planck 2018 results. X. Constraints on inflation*, *Astron. Astrophys.* **641** (2020) A10 [[1807.06211](#)].
- [12] J. Martin and V. Vennin, *Quantum Discord of Cosmic Inflation: Can we Show that CMB Anisotropies are of Quantum-Mechanical Origin?*, *Phys. Rev. D* **93** (2016) 023505 [[1510.04038](#)].
- [13] A.A. Starobinsky, *STOCHASTIC DE SITTER (INFLATIONARY) STAGE IN THE EARLY UNIVERSE*, *Lect. Notes Phys.* **246** (1986) 107.
- [14] D. Polarski and A.A. Starobinsky, *Semiclassicality and decoherence of cosmological perturbations*, *Class. Quant. Grav.* **13** (1996) 377 [[gr-qc/9504030](#)].
- [15] J. Lesgourgues, D. Polarski and A.A. Starobinsky, *Quantum to classical transition of cosmological perturbations for nonvacuum initial states*, *Nucl. Phys. B* **497** (1997) 479 [[gr-qc/9611019](#)].

[16] C. Kiefer, D. Polarski and A.A. Starobinsky, *Quantum to classical transition for fluctuations in the early universe*, *Int. J. Mod. Phys. D* **7** (1998) 455 [[gr-qc/9802003](#)].

[17] C. Kiefer and D. Polarski, *Why do cosmological perturbations look classical to us?*, *Adv. Sci. Lett.* **2** (2009) 164 [[0810.0087](#)].

[18] R. de Putter and O. Doré, *In search of an observational quantum signature of the primordial perturbations in slow-roll and ultraslow-roll inflation*, *Phys. Rev. D* **101** (2020) 043511 [[1905.01394](#)].

[19] L.P. Grishchuk and Y.V. Sidorov, *Squeezed quantum states of relic gravitons and primordial density fluctuations*, *Phys. Rev. D* **42** (1990) 3413.

[20] J. Grain and V. Vennin, *Canonical transformations and squeezing formalism in cosmology*, *JCAP* **02** (2020) 022 [[1910.01916](#)].

[21] I. Agullo, B. Bonga and P.R. Metidieri, *Does inflation squeeze cosmological perturbations?*, *JCAP* **09** (2022) 032 [[2203.07066](#)].

[22] C.P. Burgess, R. Holman, G. Kaplanek, J. Martin and V. Vennin, *Minimal decoherence from inflation*, *JCAP* **07** (2023) 022 [[2211.11046](#)].

[23] J.W. Sharman and G.D. Moore, *Decoherence due to the Horizon after Inflation*, *JCAP* **11** (2007) 020 [[0708.3353](#)].

[24] E. Joos and H.D. Zeh, *The Emergence of classical properties through interaction with the environment*, *Z. Phys. B* **59** (1985) 223.

[25] W.H. Zurek, *Pointer basis of quantum apparatus: Into what mixture does the wave packet collapse?*, *Phys. Rev. D* **24** (1981) 1516.

[26] R.H. Brandenberger, R. Laflamme and M. Mijic, *Classical Perturbations From Decoherence of Quantum Fluctuations in the Inflationary Universe*, *Mod. Phys. Lett. A* **5** (1990) 2311.

[27] F.C. Lombardo and D. Lopez Nacir, *Decoherence during inflation: The Generation of classical inhomogeneities*, *Phys. Rev. D* **72** (2005) 063506 [[gr-qc/0506051](#)].

[28] C.P. Burgess, R. Holman and D. Hoover, *Decoherence of inflationary primordial fluctuations*, *Phys. Rev. D* **77** (2008) 063534 [[astro-ph/0601646](#)].

[29] P. Martineau, *On the decoherence of primordial fluctuations during inflation*, *Class. Quant. Grav.* **24** (2007) 5817 [[astro-ph/0601134](#)].

[30] E. Nelson, *Quantum Decoherence During Inflation from Gravitational Nonlinearities*, *JCAP* **03** (2016) 022 [[1601.03734](#)].

[31] S. Shandera, N. Agarwal and A. Kamal, *Open quantum cosmological system*, *Phys. Rev. D* **98** (2018) 083535 [[1708.00493](#)].

[32] J. Martin and V. Vennin, *Observational constraints on quantum decoherence during inflation*, *JCAP* **05** (2018) 063 [[1801.09949](#)].

[33] J. Martin and V. Vennin, *Non Gaussianities from Quantum Decoherence during Inflation*, *JCAP* **06** (2018) 037 [[1805.05609](#)].

[34] J. Martin, A. Micheli and V. Vennin, *Discord and decoherence*, *JCAP* **04** (2022) 051 [[2112.05037](#)].

[35] T. Colas, J. Grain and V. Vennin, *Benchmarking the cosmological master equations*, *Eur. Phys. J. C* **82** (2022) 1085 [[2209.01929](#)].

[36] T. Colas, J. Grain and V. Vennin, *Quantum recoherence in the early universe*, *EPL* **142** (2023) 69002 [[2212.09486](#)].

[37] A. Daddi Hammou and N. Bartolo, *Cosmic decoherence: primordial power spectra and non-Gaussianities*, *JCAP* **04** (2023) 055 [[2211.07598](#)].

[38] F. Lopez and N. Bartolo, *Quantum signatures and decoherence during inflation from deep subhorizon perturbations*, [2503.23150](#).

[39] D. Sudarsky, *Shortcomings in the Understanding of Why Cosmological Perturbations Look Classical*, *Int. J. Mod. Phys. D* **20** (2011) 509 [[0906.0315](#)].

[40] J. Martin, V. Vennin and P. Peter, *Cosmological Inflation and the Quantum Measurement Problem*, *Phys. Rev. D* **86** (2012) 103524 [[1207.2086](#)].

[41] E.A. Lim, *Quantum information of cosmological correlations*, *Phys. Rev. D* **91** (2015) 083522 [[1410.5508](#)].

[42] D. Campo and R. Parentani, *Inflationary spectra and violations of Bell inequalities*, *Phys. Rev. D* **74** (2006) 025001 [[astro-ph/0505376](#)].

[43] J. Maldacena, *A model with cosmological Bell inequalities*, *Fortsch. Phys.* **64** (2016) 10 [[1508.01082](#)].

[44] J. Martin and V. Vennin, *Bell inequalities for continuous-variable systems in generic squeezed states*, *Phys. Rev. A* **93** (2016) 062117 [[1605.02944](#)].

[45] S. Choudhury, S. Panda and R. Singh, *Bell violation in the Sky*, *Eur. Phys. J. C* **77** (2017) 60 [[1607.00237](#)].

[46] J. Martin and V. Vennin, *Obstructions to Bell CMB Experiments*, *Phys. Rev. D* **96** (2017) 063501 [[1706.05001](#)].

[47] S. Kanno and J. Soda, *Infinite violation of Bell inequalities in inflation*, *Phys. Rev. D* **96** (2017) 083501 [[1705.06199](#)].

[48] J. Martin and V. Vennin, *Leggett-Garg Inequalities for Squeezed States*, *Phys. Rev. A* **94** (2016) 052135 [[1611.01785](#)].

[49] K. Ando and V. Vennin, *Bipartite temporal Bell inequalities for two-mode squeezed states*, *Phys. Rev. A* **102** (2020) 052213 [[2007.00458](#)].

[50] D. Green and R.A. Porto, *Signals of a Quantum Universe*, *Phys. Rev. Lett.* **124** (2020) 251302 [[2001.09149](#)].

[51] D. Green and Y. Huang, *Flat space analog for the quantum origin of structure*, *Phys. Rev. D* **106** (2022) 023531 [[2203.10042](#)].

[52] A. Belfiglio, R. Franzosi and O. Luongo, *Multipartite entanglement features of primordial non-gaussianities*, [2511.23389](#).

[53] J. Martin and V. Vennin, *Real-space entanglement of quantum fields*, *Phys. Rev. D* **104** (2021) 085012 [[2106.14575](#)].

[54] J.é. Martin and V. Vennin, *Real-space entanglement in the Cosmic Microwave Background*, *JCAP* **10** (2021) 036 [[2106.15100](#)].

[55] L. Espinosa-Portalés and V. Vennin, *Real-space Bell inequalities in de Sitter*, *JCAP* **07** (2022) 037 [[2203.03505](#)].

[56] I. Agullo, B. Bonga, P. Ribes-Metidieri, D. Kranas and S. Nadal-Gisbert, *How ubiquitous is entanglement in quantum field theory?*, *Phys. Rev. D* **108** (2023) 085005 [[2302.13742](#)].

[57] K. Boutivas, D. Katsinis, G. Pastras and N. Tetradis, *Entanglement in cosmology*, *JCAP* **04** (2024) 017 [[2310.17208](#)].

[58] A. Belfiglio, O. Luongo and S. Mancini, *Quantum entanglement in cosmology*, *Phys. Rept.* **1146** (2025) 1 [[2506.03841](#)].

[59] I. Agullo, B. Bonga and P. Ribes-Metidieri, *Inflation does not create entanglement in local observables*, *Class. Quant. Grav.* **43** (2026) 01LT01 [[2409.16366](#)].

[60] P. Ribes Metidieri, *Entangling Stories: Exploring Finite-Dimensional Subsystems in Curved Spacetimes Using Relativistic Quantum Information*, Ph.D. thesis, Nijmegen U., 2025.

[61] P. Ribes-Metidieri, I. Agullo and B. Bonga, *Entanglement and correlations between local observables in de Sitter spacetime*, [2511.17382](#).

[62] I. Agullo, E. Martín-Martínez, S. Nadal-Gisbert, P. Ribes-Metidieri and K. Yamaguchi, *Correlation and Entanglement partners in Gaussian systems*, [2512.11055](#).

[63] E. Wigner, *On the quantum correction for thermodynamic equilibrium*, *Phys. Rev.* **40** (1932) 749.

[64] W.B. Case, *Wigner functions and Weyl transforms for pedestrians*, *American Journal of Physics* **76** (2008) 937.

[65] J.S. BELL, *Epr correlations and epw distributions*, *Annals of the New York Academy of Sciences* **480** (1986) 263 [<https://nyaspubs.onlinelibrary.wiley.com/doi/10.1111/j.1749-6632.1986.tb12429.x>].

[66] M. Revzen, P.A. Mello, A. Mann and L.M. Johansen, *Bell's inequality violation with non-negative wigner functions*, *Phys. Rev. A* **71** (2005) 022103.

[67] M. Revzen, *The wigner function as distribution function*, *Foundations of Physics* **36** (2006) 546.

[68] J. Martin, *Cosmic Inflation, Quantum Information and the Pioneering Role of John S Bell in Cosmology*, *Universe* **5** (2019) 92 [[1904.00083](#)].

[69] A. Kenfack and K. Życzkowski, *Negativity of the Wigner function as an indicator of non-classicality*, *J. Opt. B* **6** (2004) 396.

[70] F. Albarelli, M.G. Genoni, M.G.A. Paris and A. Ferraro, *Resource theory of quantum non-Gaussianity and Wigner negativity*, *Phys. Rev. A* **98** (2018) 052350 [[1804.05763](#)].

[71] R. Hudson, *When is the wigner quasi-probability density non-negative?*, *Reports on Mathematical Physics* **6** (1974) 249.

[72] F. Soto and P. Claverie, *When is the Wigner function of multidimensional systems nonnegative?*, *Journal of Mathematical Physics* **24** (1983) 97.

[73] C. Cheung, P. Creminelli, A.L. Fitzpatrick, J. Kaplan and L. Senatore, *The Effective Field Theory of Inflation*, *JHEP* **03** (2008) 014 [[0709.0293](#)].

[74] D. Baumann and D. Green, *Equilateral Non-Gaussianity and New Physics on the Horizon*, *JCAP* **09** (2011) 014 [[1102.5343](#)].

[75] D. Green, K. Gupta and Y. Huang, *A Goldstone boson equivalence for inflation*, *JHEP* **09** (2024) 117 [[2403.05274](#)].

[76] H. Firouzjahi and B. Nikbakht, *Hamiltonians to all Orders in Perturbation Theory and Higher Loop Corrections in Single Field Inflation with PBHs Formation*, [2502.10287](#).

[77] P. Creminelli, S. Renaux-Petel, G. Tambalo and V. Yingcharoenrat, *Non-perturbative wavefunction of the universe in inflation with (resonant) features*, *JHEP* **03** (2024) 010 [[2401.10212](#)].

[78] J.M. Maldacena, *Non-Gaussian features of primordial fluctuations in single field inflationary models*, *JHEP* **05** (2003) 013 [[astro-ph/0210603](#)].

[79] C. Cheung, A.L. Fitzpatrick, J. Kaplan and L. Senatore, *On the consistency relation of the 3-point function in single field inflation*, *JCAP* **02** (2008) 021 [[0709.0295](#)].

[80] S.R. Behbahani, A. Dymarsky, M. Mirbabayi and L. Senatore, *(Small) Resonant non-Gaussianities: Signatures of a Discrete Shift Symmetry in the Effective Field Theory of Inflation*, *JCAP* **12** (2012) 036 [[1111.3373](#)].

[81] J.-L. Lagrange, *Nouvelle méthode pour résoudre des équations littérales par les moyen des séries*, *Mém. Acad. Roy. Sci. Belles-Lettres de Berlin* (1770) .

[82] I.M. Gessel, *Lagrange inversion*, *Journal of Combinatorial Theory, Series A* **144** (2016) 212.

[83] A.A. Starobinsky, *Dynamics of Phase Transition in the New Inflationary Universe Scenario and Generation of Perturbations*, *Phys. Lett. B* **117** (1982) 175.

[84] A.A. Starobinsky, *Multicomponent de Sitter (Inflationary) Stages and the Generation of Perturbations*, *JETP Lett.* **42** (1985) 152.

[85] M. Sasaki and E.D. Stewart, *A General analytic formula for the spectral index of the density perturbations produced during inflation*, *Prog. Theor. Phys.* **95** (1996) 71 [[astro-ph/9507001](#)].

[86] M. Sasaki and T. Tanaka, *Superhorizon scale dynamics of multiscalar inflation*, *Prog. Theor. Phys.* **99** (1998) 763 [[gr-qc/9801017](#)].

[87] D.H. Lyth, K.A. Malik and M. Sasaki, *A General proof of the conservation of the curvature perturbation*, *JCAP* **05** (2005) 004 [[astro-ph/0411220](#)].

[88] T. Fujita, M. Kawasaki, Y. Tada and T. Takesako, *A new algorithm for calculating the curvature perturbations in stochastic inflation*, *JCAP* **12** (2013) 036 [[1308.4754](#)].

[89] T. Fujita, M. Kawasaki and Y. Tada, *Non-perturbative approach for curvature perturbations in stochastic δN formalism*, *JCAP* **10** (2014) 030 [[1405.2187](#)].

[90] V. Vennin and A.A. Starobinsky, *Correlation Functions in Stochastic Inflation*, *Eur. Phys. J. C* **75** (2015) 413 [[1506.04732](#)].

[91] D.S. Salopek and J.R. Bond, *Nonlinear evolution of long-wavelength metric fluctuations in inflationary models*, *Phys. Rev. D* **42** (1990) 3936.

[92] D. Wands, K.A. Malik, D.H. Lyth and A.R. Liddle, *A New approach to the evolution of cosmological perturbations on large scales*, *Phys. Rev. D* **62** (2000) 043527 [[astro-ph/0003278](#)].

[93] D.H. Lyth and D. Wands, *Conserved cosmological perturbations*, *Phys. Rev. D* **68** (2003) 103515 [[astro-ph/0306498](#)].

[94] G.I. Rigopoulos and E.P.S. Shellard, *The separate universe approach and the evolution of nonlinear superhorizon cosmological perturbations*, *Phys. Rev. D* **68** (2003) 123518 [[astro-ph/0306620](#)].

[95] D.H. Lyth and Y. Rodriguez, *The Inflationary prediction for primordial non-Gaussianity*, *Phys. Rev. Lett.* **95** (2005) 121302 [[astro-ph/0504045](#)].

[96] P.J. Steinhardt and M.S. Turner, *A Prescription for Successful New Inflation*, *Phys. Rev. D* **29** (1984) 2162.

[97] A.R. Liddle and D.H. Lyth, *COBE, gravitational waves, inflation and extended inflation*, *Phys. Lett. B* **291** (1992) 391 [[astro-ph/9208007](#)].

[98] A.R. Liddle, P. Parsons and J.D. Barrow, *Formalizing the slow roll approximation in inflation*, *Phys. Rev. D* **50** (1994) 7222 [[astro-ph/9408015](#)].

[99] J. Martin, C. Ringeval and V. Vennin, *Encyclopædia Inflationaris: Opiparous Edition*, *Phys. Dark Univ.* **5-6** (2014) 75 [[1303.3787](#)].

[100] W.H. Kinney, *Horizon crossing and inflation with large eta*, *Phys. Rev. D* **72** (2005) 023515 [[gr-qc/0503017](#)].

[101] J. Martin, H. Motohashi and T. Suyama, *Ultra Slow-Roll Inflation and the non-Gaussianity Consistency Relation*, *Phys. Rev. D* **87** (2013) 023514 [[1211.0083](#)].

[102] M.H. Namjoo, H. Firouzjahi and M. Sasaki, *Violation of non-Gaussianity consistency relation in a single field inflationary model*, *EPL* **101** (2013) 39001 [[1210.3692](#)].

[103] K. Dimopoulos, *Ultra slow-roll inflation demystified*, *Phys. Lett. B* **775** (2017) 262 [[1707.05644](#)].

[104] C. Pattison, V. Vennin, H. Assadullahi and D. Wands, *The attractive behaviour of ultra-slow-roll inflation*, *JCAP* **08** (2018) 048 [[1806.09553](#)].

[105] D. Wands, *Duality invariance of cosmological perturbation spectra*, *Phys. Rev. D* **60** (1999) 023507 [[gr-qc/9809062](#)].

[106] M. Kleber, *Exact solutions for time-dependent phenomena in quantum mechanics*, *Physics Reports* **236** (1994) 331.

[107] A. Anderson, *Canonical Transformations in Quantum Mechanics*, *Annals Phys.* **232** (1994) 292 [[hep-th/9305054](#)].

[108] V. Briaud, A. Karam, N. Koivunen, E. Tomberg, H. Veermäe and V. Vennin, *How deep is the dip and how tall are the wiggles in inflationary power spectra?*, *JCAP* **05** (2025) 097 [[2501.14681](#)].

[109] M. Moshinsky and C. Quesne, *Linear canonical transformations and their unitary representations*, *J. Math. Phys.* **12** (1971) 1772.

[110] M. Blaszak and Z. Domanski, *Canonical transformations in quantum mechanics*, [1208.2835](#).

[111] J.H.P. Jackson, H. Assadullahi, A.D. Gow, K. Koyama, V. Vennin and D. Wands, *The separate-universe approach and sudden transitions during inflation*, *JCAP* **05** (2024) 053 [[2311.03281](#)].

[112] D.H. Lyth, K.A. Malik and M. Sasaki, *A General proof of the conservation of the curvature perturbation*, *JCAP* **05** (2005) 004 [[astro-ph/0411220](#)].

[113] V.V. Dodonov, I.A. Malkin and V.I. Man'ko, *Even and odd coherent states and excitations of a singular oscillator*, *Physica* **72** (1974) 597.

- [114] K. Takase, J.-i. Yoshikawa, W. Asavanant, M. Endo and A. Furusawa, *Generation of optical Schrödinger's cat states by generalized photon subtraction*, *Phys. Rev. A* **103** (2021) 013710 [[2009.08580](https://arxiv.org/abs/2009.08580)].
- [115] “NIST Digital Library of Mathematical Functions.” <https://dlmf.nist.gov/>, Release 1.2.5 of 2025-12-15.
- [116] E.M. Ferreira and J. Sesma, *Zeros of the Macdonald function of complex order*, *Journal of Computational and Applied Mathematics* **211** (2008) 223 [[math/0607471](https://arxiv.org/abs/math/0607471)].
- [117] S.M. Leach, M. Sasaki, D. Wands and A.R. Liddle, *Enhancement of superhorizon scale inflationary curvature perturbations*, *Phys. Rev. D* **64** (2001) 023512 [[astro-ph/0101406](https://arxiv.org/abs/astro-ph/0101406)].
- [118] D. Artigas, S. Pi and T. Tanaka, *Extended δN Formalism: Nonspatially Flat Separate-Universe Approach*, *Phys. Rev. Lett.* **134** (2025) 221001 [[2408.09964](https://arxiv.org/abs/2408.09964)].
- [119] V. Briaud, R. Kawaguchi and V. Vennin, *Stochastic inflation with gradient interactions*, *JCAP* **12** (2025) 024 [[2509.05124](https://arxiv.org/abs/2509.05124)].
- [120] S.A. Salcedo, T. Colas and E. Pajer, *The open effective field theory of inflation*, *JHEP* **10** (2024) 248 [[2404.15416](https://arxiv.org/abs/2404.15416)].
- [121] R. Christie, J. Joo, G. Kaplanek, V. Vennin and D. Wands, *Cosmic Lockdown: When Decoherence Saves the Universe from Tunneling*, [2512.14204](https://arxiv.org/abs/2512.14204).
- [122] H. Goldstein, C. Poole and J. Safko, *Classical Mechanics*, Addison Wesley (2002).
- [123] M. Braglia and L. Pinol, *No time to derive: unraveling total time derivatives in in-in perturbation theory*, *JHEP* **08** (2024) 068 [[2403.14558](https://arxiv.org/abs/2403.14558)].